

Rational Design of CT-coupled J-Aggregation Platform based on Aza-BODIPY for Highly Efficient Phototherapy

Shengmei Wu,[†] Wenze Zhang,[†] Chaoran Li^b, Zhigang Ni,^a Weifeng Chen,^a Lizhi Gai,^{*a} Jiangwei Tian,^{*b} Zijian Guo^c and Hua Lu^{*a}

Table of Contents

I. Experimental Section

I.1 Methods and materials.....	S2
I.2 Synthesis.....	S3-S5
I.3 TD-DFT calculations.....	S6
I.4 Spectroscopic measurements.....	S7
I.5 Preparation of nanoparticle.....	S8-S10
I.6 PTT properties of dyes.....	S11
I.7 PDT properties of BDP1-2 NPs.....	S12
I.8 General animals culture.....	S13-S15
II. ¹ H NMR, ¹³ C NMR spectra and HR-MS	S16-S30
III. Cartesian coordinates.....	S31-S39
IV. References.....	S40

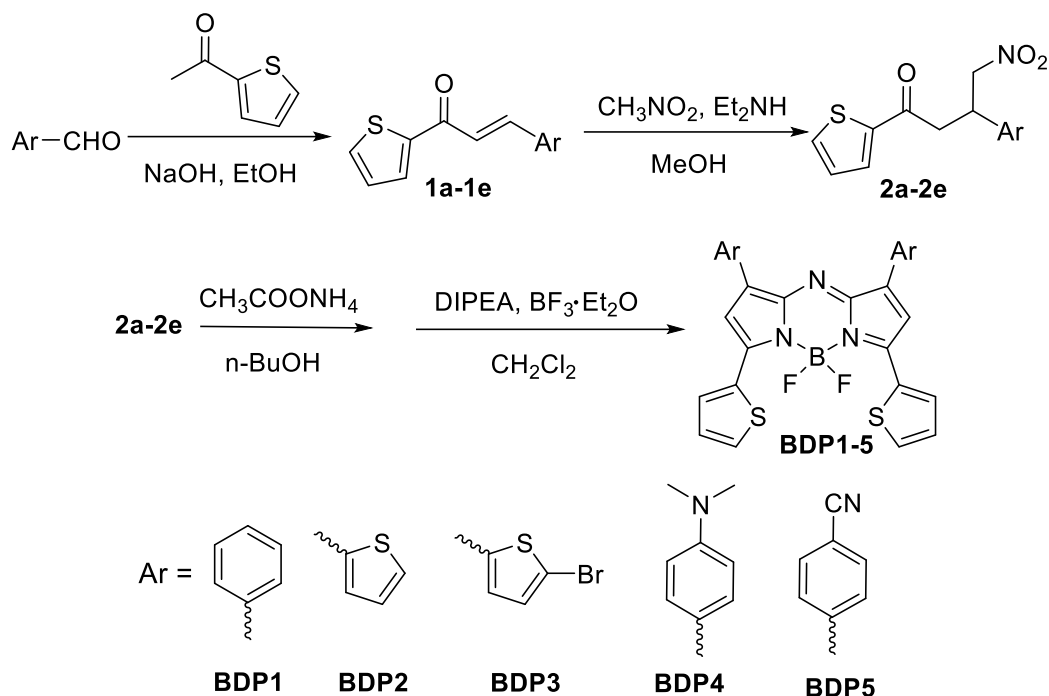
Experimental Procedures

I. 1 Methods and materials

All reactions were carried out under a dry argon atmosphere by using Schlenk techniques. All reagents were obtained from commercial suppliers and used without further purification unless otherwise indicated. All air- and moisture-sensitive reactions were carried out under a nitrogen atmosphere. Glassware was dried in an oven at 100°C and cooled under a stream of inert gas before use. Dichloromethane was distilled over calcium hydride. All the solvents employed for the spectroscopic measurements were of spectroscopic grade. Analytical thin-layer chromatography was performed on glass plates coated with 0.25 mm 250–400 mesh silica gel containing a fluorescent indicator (Merck). Flash column chromatography (200 mesh) was carried out using silica gel purchased from Qingdao Haiyang Silica Gel Co.

¹H NMR, ¹³C NMR spectra were recorded on a Bruker DRX400 / 500 spectrometer and referenced to the residual proton signals of the solvent, reporting chemical shifts in ppm compared to SiMe₄. The ¹H NMR coupling constants (J) are reported in Hertz (Hz) and the multiplicity is expressed as follows: s (singlet), d (doublet), m (multiplet). HR-MS were recorded on a Bruker Daltonics microTOF-Q II spectrometer. UV-visible absorption spectra and fluorescence emission spectra were recorded on a commercial spectrophotometer (Shimadzu UV-1800 and Horiba JobinYvonFluorolog-3 spectrofluorometers) at room temperature. The diameter of the nanoparticles was determined by dynamic light scattering (DLS) on a Zetasizer Nano ZSE (Malvern, UK) with a semiconductor laser (50 nW) as a light source. Confocal laser scanning microscope (CLSM) images were performed on Zeiss LSM710 confocal laser scanning microscope. The PA signals of disease areas were measured by Visualsonic Vevo 2100 LAZER system. Photothermal effects were determined using a UNI-T UT325 thermometer. Infrared (IR) thermal imaging was performed using a FLIR E53 thermal imaging camera.

I.2 Synthesis



General synthetic method for 1a-1e

To a solution of benzaldehyde (5.0 g, 42 mmol) and 2-acetylthiophene (4.7 g, 42 mmol) in ethanol (50 mL) were added an aqueous solution of sodium hydroxide (8.4 g, 210 mmol, 10 mL water) under ice bath conditions. The mixture was stirred at room temperature for 12 h. After the reaction is complete, the products precipitated were filtered, washed with aqueous ethanol, and dried in a vacuum. **1a**, white solid (93% yield). ¹H NMR (400 MHz, CDCl₃) δ 7.88–7.84 (m, 2H), 7.69–7.68 (m, 1H), 7.66–7.64 (m, 2H), 7.45–7.41 (m, 4H), 7.19 (dd, *J* = 4 Hz, 1H). ¹³C NMR (101 MHz, CDCl₃) δ 182.2, 145.6, 144.2, 134.8, 134.1, 132.0, 130.7, 129.1, 128.6, 128.4, 121.7.

1b, white solid (88% yield). ¹H NMR (400 MHz, CDCl₃) δ 8.01–7.97 (m, 1H), 7.87 (dd, *J* = 4 Hz, 1H), 7.70 (dd, *J* = 8, 4 Hz, 1H), 7.45 (d, *J* = 8 Hz, 1H), 7.39 (d, *J* = 4 Hz, 1H), 7.22–7.19 (m, 2H), 7.13–7.11 (m, 1H). ¹³C NMR (101 MHz, CDCl₃) δ 189.8, 143.7, 138.9, 134.5, 132.4, 129.2, 128.4, 128.1, 127.6, 79.5.

1c, white solid (75% yield). ¹H NMR (400 MHz, CDCl₃) δ 7.84–7.80 (m, 2H), 7.68 (dd, *J* = 4 Hz, 1H), 7.18 (dd, *J* = 4 Hz, 1H), 7.11–7.09 (m, 1H), 7.07 (s, 1H), 7.05 (d, *J* = 4 Hz, 1H). ¹³C NMR (101 MHz, CDCl₃) δ 181.4, 145.4, 141.8, 135.6, 134.2, 132.6, 131.9, 131.5, 128.4, 120.7, 116.6.

1d, yellow solid (78% yield). ¹H NMR (400 MHz, CDCl₃) δ 7.88 (d, *J* = 8, 4 Hz, 2H), 7.67 (d, *J* = 4 Hz, 1H), 7.59 (d, *J* = 8 Hz, 2H), 7.30–7.29 (m, 1H), 7.20 (t, *J* = 4 Hz, 1H), 6.73 (d, *J* = 8 Hz, 2H), 3.08 (s, 6H). ¹³C NMR (101 MHz, CDCl₃) δ 182.2, 152.2, 146.5, 145.1, 133.0, 131.0, 130.6, 128.2, 122.5, 116.4, 111.9, 40.2.

1e, white solid (91% yield). ¹H NMR (400 MHz, CDCl₃) δ 7.87 (d, *J* = 4 Hz, 1H), 7.79–7.75 (m, 1H), 7.70 (d, *J* = 4 Hz, 1H), 7.56–7.48 (m, 4H), 7.42–7.38 (m, 1H), 7.18 (t, *J* = 8 Hz, 1H). ¹³C NMR (101 MHz, CDCl₃) δ 181.4, 145.1, 141.5, 139.1, 134.8, 132.8, 132.4, 128.9, 128.6, 124.8, 118.5, 113.7.

General synthetic method for 2a-2e

Compound **1a** (5.0 g, 23 mmol), nitromethane (8.8 mL, 184 mmol), and diethylamine (18.9 mL, 184 mmol) were dissolved in ethanol (50 mL), and the mixture was refluxed for 3 hours. After cooling to room temperature, the resulting mixture was evaporated to dryness and then dissolved in ethyl acetate. The mixture was washed with water and brine, dried with sodium sulfate, and concentrated to give the crude product. Purification by column chromatography (EA: PE = 1:4) yields the desired products. **2a**, yellow oily liquid (76%). ¹H NMR (400 MHz, CDCl₃)

δ 7.72 (dd, $J = 4$ Hz, 1H), 7.68 (dd, $J = 4$ Hz, 1H), 7.38–7.34 (m, 2H), 7.31–7.28 (m, 3H), 7.15 (dd, $J = 4$ Hz, 1H), 4.89–4.84 (m, 1H), 4.75–4.70 (m, 1H), 4.27–4.19 (m, 1H), 3.48–3.34 (m, 2H). ^{13}C NMR (101 MHz, CDCl_3) δ 141.5, 138.6, 129.0, 128.8, 128.5, 128.4, 128.2, 126.7, 125.9, 124.1, 122.4, 38.1, 24.7, 17.6.

The synthesis method of compound **2b** is the same as that of **2a**. **2b**, yellow oily liquid (72%). ^1H NMR (500 MHz, CDCl_3) δ 7.73 (d, $J = 4$ Hz, 1H), 7.67 (d, $J = 4$ Hz, 1H), 7.20 (d, $J = 4$ Hz, 1H), 7.14 (t, $J = 4$ Hz, 1H), 6.96–6.92 (m, 2H), 4.86 (dd, $J = 8, 4$ Hz, 1H), 4.73 (dd, $J = 8, 4$ Hz, 1H), 4.55–4.49 (m, 1H), 3.49–3.39 (m, 2H). ^{13}C NMR (101 MHz, CDCl_3) δ 189.4, 143.5, 141.6, 134.7, 132.6, 128.5, 127.3, 125.8, 124.9, 79.8, 42.9, 35.0.

The synthesis method of compound **2c** is the same as that of **2a**. **2c**, yellow oily liquid (62%). ^1H NMR (400 MHz, CDCl_3) δ 7.72 (d, $J = 4$ Hz, 1H), 7.68 (d, $J = 4$ Hz, 1H), 7.21 (d, $J = 4$ Hz, 1H), 7.14–7.13 (m, 1H), 7.96–7.92 (m, 2H), 6.72 (d, $J = 4$ Hz, 1H), 4.85 (dd, $J = 8, 4$ Hz, 1H), 4.72 (dd, $J = 8, 4$ Hz, 1H), 4.55–4.49 (m, 1H), 3.39–3.49 (m, 2H). ^{13}C NMR (101 MHz, CDCl_3) δ 189.0, 143.2, 134.9, 132.6, 130.1, 130.0, 128.5, 126.4, 111.6, 79.4, 42.5, 35.3.

Synthesis of compound **2d** is the same as that of **2a**. **2d**, yellow oily liquid (63%). ^1H NMR (400 MHz, CDCl_3) δ 7.70 (dd, $J = 4$ Hz, 1H), 7.65 (dd, $J = 4$ Hz, 1H), 7.14–7.11 (m, 3H), 6.68 (d, $J = 8$ Hz, 2H), 4.81–4.76 (m, 1H), 4.67–4.62 (m, 1H), 4.13–4.06 (m, 1H), 3.40–3.28 (m, 2H), 2.92 (s, 6H). ^{13}C NMR (101 MHz, CDCl_3) δ 190.2, 150.0, 143.8, 134.3, 132.3, 128.3, 128.2, 126.2, 112.9, 79.9, 42.5, 40.6, 38.9.

The synthesis method of compound **2e** is the same as that of **2a**. **2e**, yellow oily liquid (75%). ^1H NMR (400 MHz, CDCl_3) δ 7.69 (dd, $J = 4$ Hz, 2H), 7.64 (d, $J = 8$ Hz, 2H), 7.42 (d, $J = 8$ Hz, 2H), 7.15–7.12 (m, 1H), 4.88–4.83 (m, 1H), 4.75–4.69 (m, 1H), 4.31–4.24 (m, 1H), 3.39 (d, $J = 8$ Hz, 2H). ^{13}C NMR (101 MHz, CDCl_3) δ 188.9, 144.3, 143.2, 134.9, 133.0, 132.5, 128.6, 128.5, 118.4, 112.2, 78.8, 41.7, 39.4.

General synthetic method for BDP1-5.

2a (1.0 g, 3.6 mmol) and ammonium acetate (9.3 g, 126 mmol) were dissolved in n-butanol (25 mL) and refluxed the mixture for 14 hours. After cooling to room temperature, the resulting precipitate was collected, and washed with water (50 mL) and EtOH (60 mL). The resulting solid was allowed to dry in the oven to obtain the products Azadipyrromethene, which were used in the next step without further purification.

To a new distilled solution of CH_2Cl_2 (60 mL), Azadipyrromethene (100 mg, 0.22 mmol) was added along with N, N-diisopropylethylamine (0.5 mL) under an ice bath. After stirring for 10 minutes, $\text{BF}_3 \cdot \text{OEt}_2$ (1.0 mL) was added carefully and the mixture was allowed to stir at room temperature for 3 h. The crude mixture was diluted with dichloromethane and washed with water and brine. The organic layer was dried over magnesium sulphate and the solvent was removed under reduced pressure. Chromatography on silica with CH_2Cl_2 afforded **BDP1** (45%) as a coppery, shining solid. ^1H NMR (400 MHz, CDCl_3) δ 8.39 (d, $J = 4$ Hz, 2H), 8.06 (dd, $J = 8, 4$ Hz, 4H), 7.65 (d, $J = 8$ Hz, 2H), 7.48–7.46 (m, 3H), 7.44–7.42 (m, 3H), 7.29–7.27 (m, 2H), 7.18 (s, 2H). HR-MS(ESI): $[\text{M}+\text{H}]^+$ calcd for $\text{C}_{28}\text{H}_{19}\text{BF}_2\text{N}_3\text{S}_2$ $m/z=510.1076$; found $m/z=510.1006$.

The synthesis of compound **BDP2** is the same as that of **BDP1**. **BDP2**, coppery, shining solid (40%). ^1H NMR (400 MHz, CDCl_3) δ 8.35 (d, $J = 4$ Hz, 2H), 7.93 (d, $J = 4$ Hz, 2H), 7.63 (d, $J = 8$ Hz, 2H), 7.57 (d, $J = 4$ Hz, 2H), 7.27 (s, 1H), 7.25 (s, 1H), 7.21–7.19 (m, 2H), 7.07 (s, 2H). HR-MS(ESI): $[\text{M}]^+$ calcd for $\text{C}_{24}\text{H}_{14}\text{BF}_2\text{N}_3\text{S}_4$ $m/z=521.0132$; found $m/z=521.0173$.

The synthesis of compound **BDP3** is the same as that of **BDP1**. **BDP3**, coppery, shining solid (32%). ^1H NMR (400 MHz, CDCl_3) δ 8.35 (t, $J = 4$ Hz, 1H), 8.30 (d, $J = 4$ Hz, 1H), 7.91 (d, $J = 4$ Hz, 1H), 7.65–7.60 (m, 3H), 7.58–7.54 (m, 2H), 7.20–7.17 (m, 1H), 7.11 (d, $J = 4$ Hz, 1H), 7.05 (s, 1H), 6.97 (s, 1H). HR-MS(ESI): $[\text{M}]^+$ calcd for $\text{C}_{24}\text{H}_{12}\text{BBr}_2\text{F}_2\text{N}_3\text{S}_4$ $m/z=676.8342$; found $m/z=676.8355$.

Compound **BDP4** was synthesized using the same method as **BDP1**. **BDP4**, coppery, shining solid (28%). ^1H NMR (400 MHz, CDCl_3) δ 8.02 (d, $J = 8$ Hz, 4H), 7.56 (d, $J = 4$ Hz, 2H), 7.45 (d, $J = 4$ Hz, 2H), 7.18–7.16 (m, 2H),

6.91 (s, 2H), 6.77 (d, $J = 8$ Hz, 4H), 3.04 (s, 12H). HR-MS(ESI): $[M+H]^+$ calcd for $C_{32}H_{29}BF_2N_5S_2$ $m/z=596.1920$; found $m/z=596.1918$.

Compound **BDP5** was synthesized using the same method as **BDP1**. **BDP5**, coppery, shining solid (33%). 1H NMR (400 MHz, $CDCl_3$) δ 8.41 (d, $J = 4$ Hz, 2H), 8.08 (d, $J = 4$ Hz, 4H), 7.75 (d, $J = 4$ Hz, 4H), 7.72 (d, $J = 4$ Hz, 2H), 7.31 (d, $J = 4$ Hz, 2H), 7.08 (s, 2H). HR-MS(ESI): $[M+H]^+$ calcd for $C_{30}H_{17}BF_2N_5S_2$ $m/z=560.0981$; found $m/z=560.0970$.

I.3 TD-DFT calculation

The ground state structures of compounds **BDP1-5** are optimized using the density functional theory (DFT) method with the B3LYP functional and 6-31G(d) basis set. The absorption properties were predicted by the time-dependent (TD-DFT) method with the same basis set. All the above computations were performed using Gaussian 16, Revision C.01.^[1]

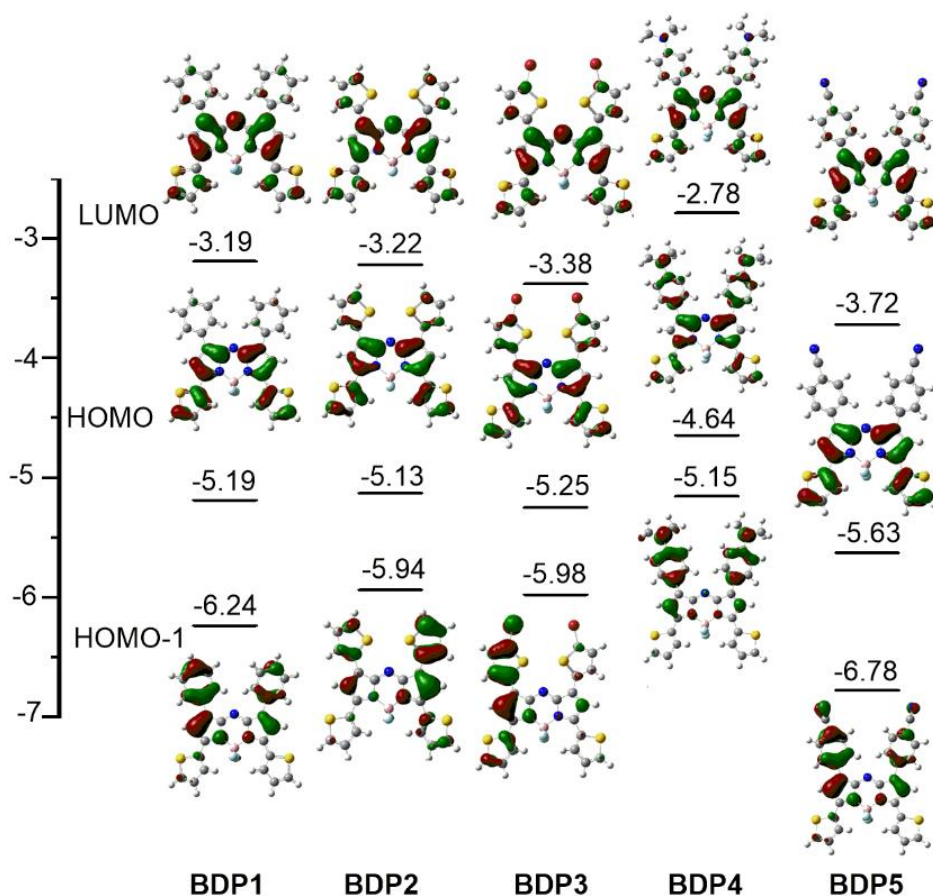


Figure S1. Calculated HOMO and LUMO energy levels of **BDP1-5** at an isosurface value of 0.035 a.u.

Table S1. Calculated electronic excitations energies, oscillator strengths and the related wave functions.

	State ^a	Energy[eV]	λ [nm]	f^b	Orbitals(coefficient) ^c
BDP1	S ₁	2.07	601	0.73	H→L (98%)
BDP2	S ₁	1.96	634	0.63	H→L (92%)
BDP3	S ₁	1.88	662	0.56	H→L (96%)
BDP4	S ₁	1.77	700	0.46	H→L (89%), H-2→L (12%)
BDP5	S ₁	1.90	652	0.59	H→L (88%), H-2→L (12%)

^a Excited state. ^b Oscillator strength. ^c MOs involved in the transitions.

I.4 Spectroscopic measurements

Table S2. Summarized spectroscopic properties of **BDP1-5** in THF at 298K.

Dyes	$\lambda_{\text{abs}}^{\text{a}}$ [nm]	$\lambda_{\text{em}}^{\text{b}}$ [nm]	$\Delta\nu^{\text{c}}$ [cm ⁻¹]	ϵ [M ⁻¹ cm ⁻¹]	$\Phi_{\text{F}}^{\text{d}}$	$\tau_{\text{F}}^{\text{e}}$ [ns]	K_{r}^{f} [10 ⁸ s ⁻¹]	K_{nr}^{g} [10 ⁸ s ⁻¹]
BDP1	717	741	452	71700	0.24	3.56	0.67	2.13
BDP2	741	763	389	75100	0.11	2.79	0.39	3.19
BDP3	746	768	384	49700	0.09	2.07	0.43	4.40
BDP4	663, 786	737(LE) ^h	1514	30500	0.01	2.81	0.04	3.52
BDP5	732	762	538	64000	0.15	3.32	0.45	2.56

^aAbsorption maximum in THF. ^bFluorescence maximum in THF. ^cStokes shift. ^dFluorescence quantum yield, the standard errors are less than 5%. ^eFluorescence lifetime. ^fRadiative rate constants were calculated $k_{\text{r}} = \Phi_{\text{F}}/\tau$. ^gNonradiative rate constants were calculated $k_{\text{nr}} = (1 - \Phi_{\text{F}})/\tau$. ^hLocal excited state.

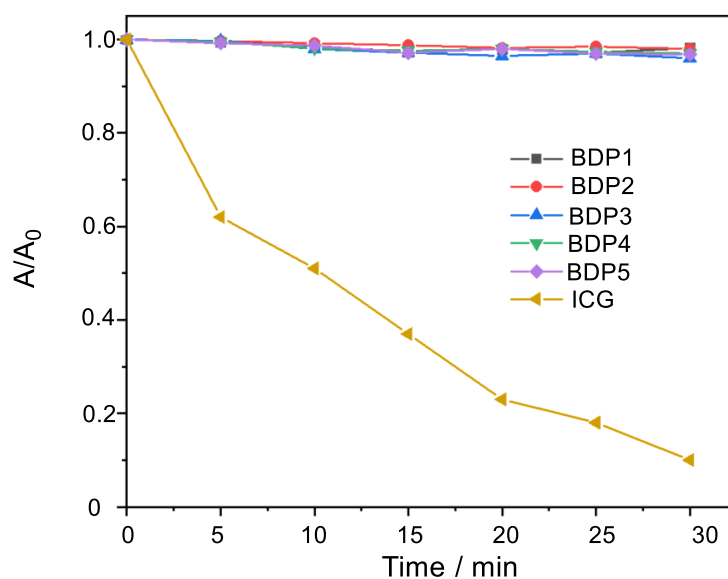


Figure S2. Comparison of the photostability of **BDP1-5** (5×10^{-5} M) and ICG (1×10^{-5} M) in DCM under continuous irradiation with a 100 W Xe lamp over 30 min; 25 mW/cm².

I.5 Preparation of nanoparticle

2 mg of **BDP** were dissolved in tetrahydrofuran (THF, 2 mL). 2 mg of DSPE-mPEG2000 were dissolved in 4 mL of ultrapure water, and sonicate for dissolution. Take 500 μL of **BDP** in THF and quickly inject it into the aqueous solution of DSPE-mPEG2000. The THF was removed by blowing nitrogen gas under a constant temperature water bath at 50° C to obtain water-soluble nanoparticles. Add the aqueous solution into an ultrafiltration centrifuge tube, perform ultrafiltration for 5 minutes under the action of a centrifuge at 3500 r/min, repeat centrifugation with ultrapure water three times to remove excess DSPE-mPEG2000, and store in a refrigerator at 4 °C.

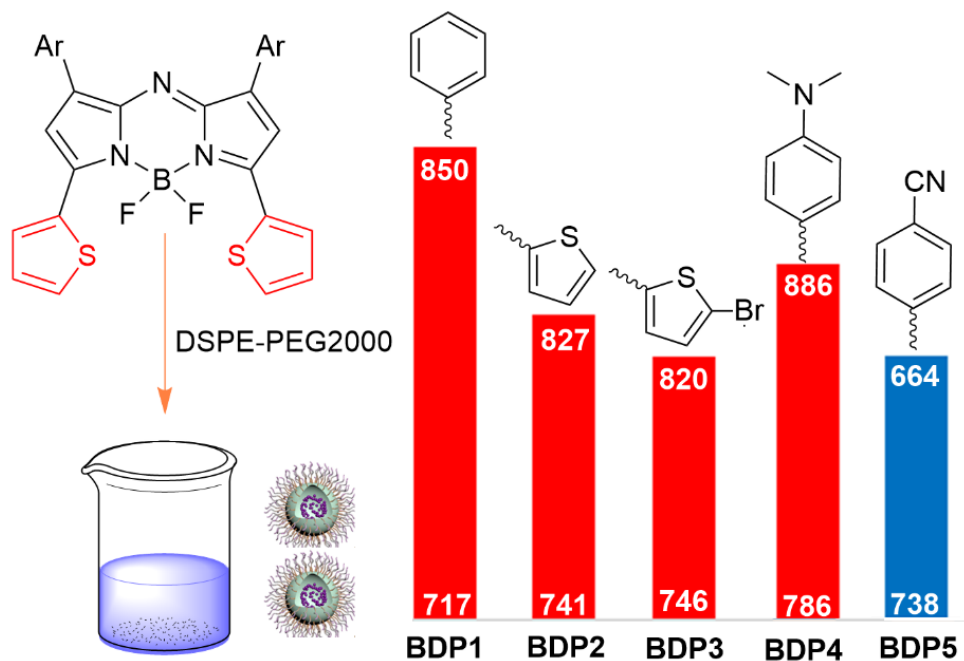


Figure S3. Comparison of absorption of **BDP1-5** in THF and **BDP1-5 NPs** in water.

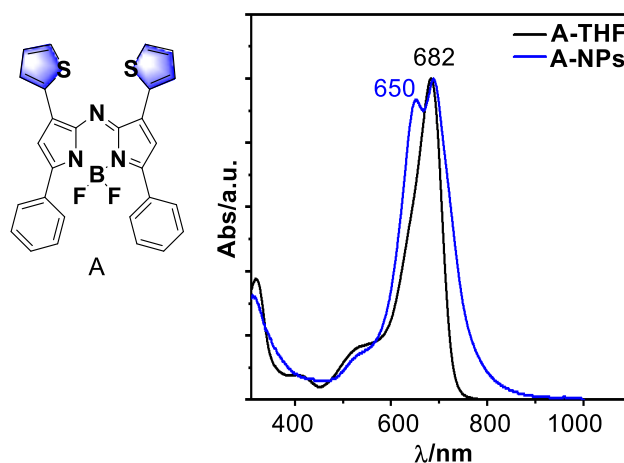


Figure S4. Structure of dye **A** (left). Comparison of absorption of **A** in THF and **A-NPs** in water (right).

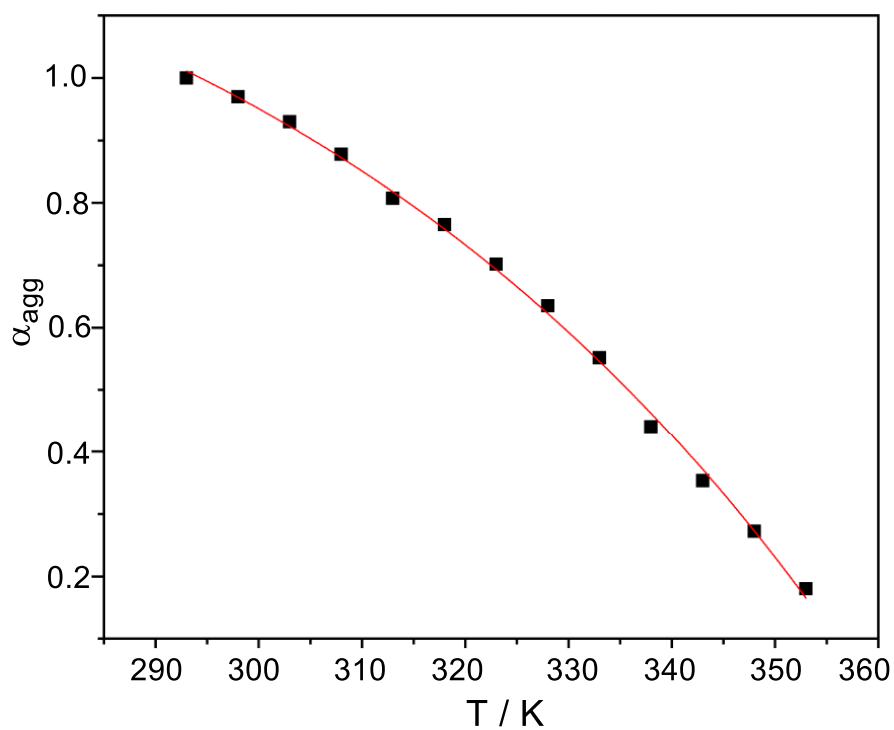


Figure S5. Plot of α_{agg} of BDP2 (10 μ M) in DMF/water (3/2) as a function of temperature for the data collected at 833 nm, and the corresponding fitting curves with the nucleation-elongation model.^[2]

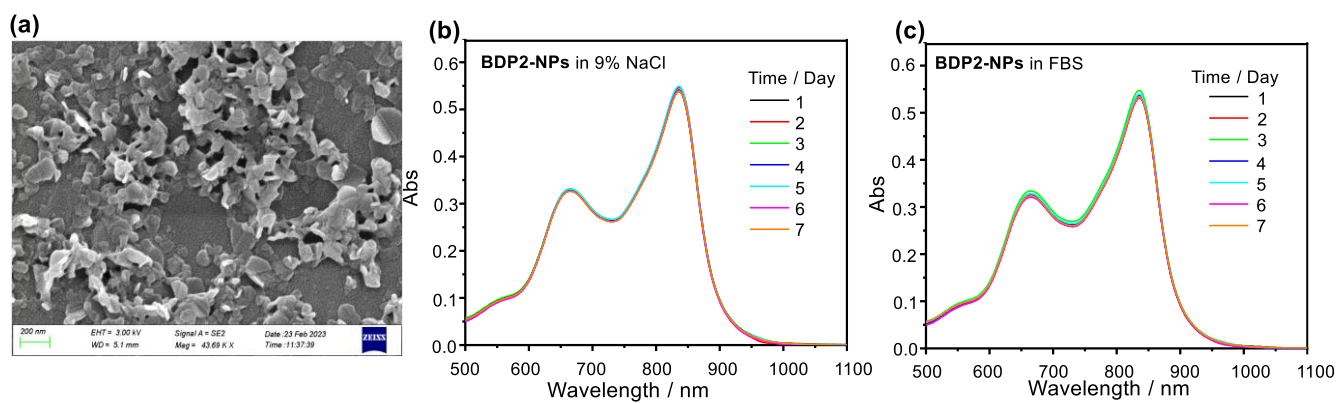


Figure S6. (a) SEM image of **BDP2** in DMF/water (3/2). (b-c) Absorption spectra of **BDP2-NPs** in 9% NaCl(b) or fetal blood serum (c) for different times.

I.6 PTT properties of dyes

Photothermal Conversion Efficiency of BDP1-2-NPs

BDP1-2-NPs in water were irradiated by 808 nm laser for 15 min and then cooled to room temperature, and the temperature of samples were recorded by an infrared camera, relatively. At the same time, pure DMF or water were used as the negative control group.

The photothermal conversion efficiencies (η) was measured and calculated according to these equations (1-4):

$$\eta = \frac{hS(T_{max} - T_{surr}) - Q_s}{I(1 - 10^{-A})} \quad (1)$$

$$\theta = \frac{\Delta T}{\Delta T_{max}} = \frac{T - T_{surr}}{T_{max} - T_{surr}} \quad (2)$$

$$t = -\tau \ln \theta \quad (3)$$

$$hS = \frac{mC_p}{\tau} \quad (4)$$

where h is the heat transfer coefficient, S is the surface area of the container. The T_{max} and T_{surr} are the maximum temperature of the solution and the ambient temperature, respectively, I is the laser power, A is the absorbance of the sample at 808 nm and Q_s expresses the heat associated with light absorption by the solvent. m and C_p are the mass and heat capacity of the system, respectively, τ is the heat transfer time constant, which can be determined by the linear relationship of t versus $-\ln \theta$ through the natural cooling curve of the sample.

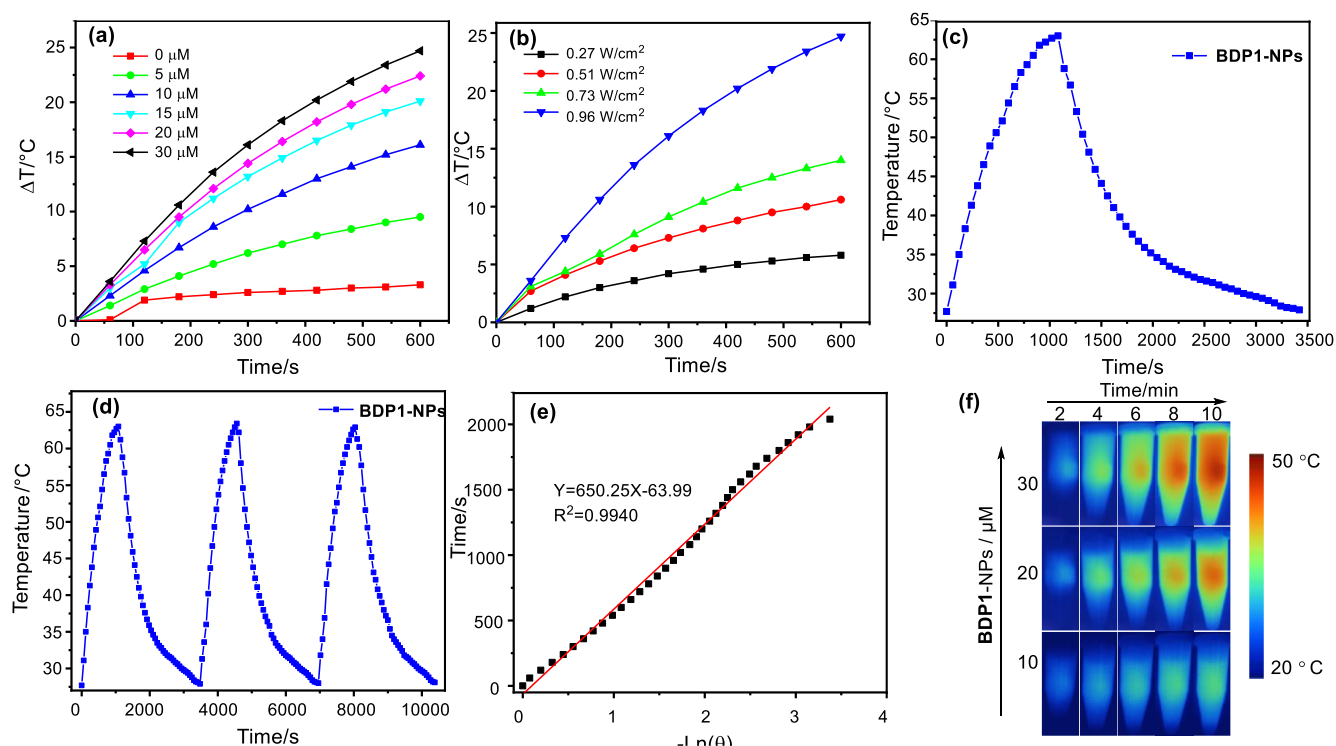


Figure S7. (a) Photothermal conversion of **BDP1-NPs** at different concentrations under 808 nm (0.96 W cm^{-2}) laser irradiation. (b) Photothermal conversion of **BDP1-NPs** ($30 \mu\text{M}$) under 808 nm laser irradiation with different exposure intensities. (c) Photothermic heating curves of the **BDP1-NPs** dispersions under 808 nm irradiation (0.96 W cm^{-2}) for 20 min followed by cooling to room temperature. (d) Photothermic stability of **BDP1-NPs** upon 808 nm laser irradiation of 0.96 W cm^{-2} for three on/off cycles. (e) Linear correlation of the cooling times versus negative natural logarithm of driving force temperatures. (f) Infrared thermal images of **BDP1-NPs** with different concentrations upon exposure to the NIR laser (808 nm, 0-10 min) at a power density of 0.96 W cm^{-2} .

I.7 PDT properties of BDP1-2 NPs

For singlet oxygen detection, 1.0 mg of ABDA was accurately weighed and dissolved in sodium hydroxide (2 mg/mL, 1 mL), 10 μ L of ABDA sodium salt was added to **BDP1-2** NPs (10 μ M). The UV-vis absorption spectra of ABDA sodium salt aqueous solution in the absence and presence of **BDP1-2** were recorded every 15s under 808 nm laser irradiation (0.96 W/cm²).

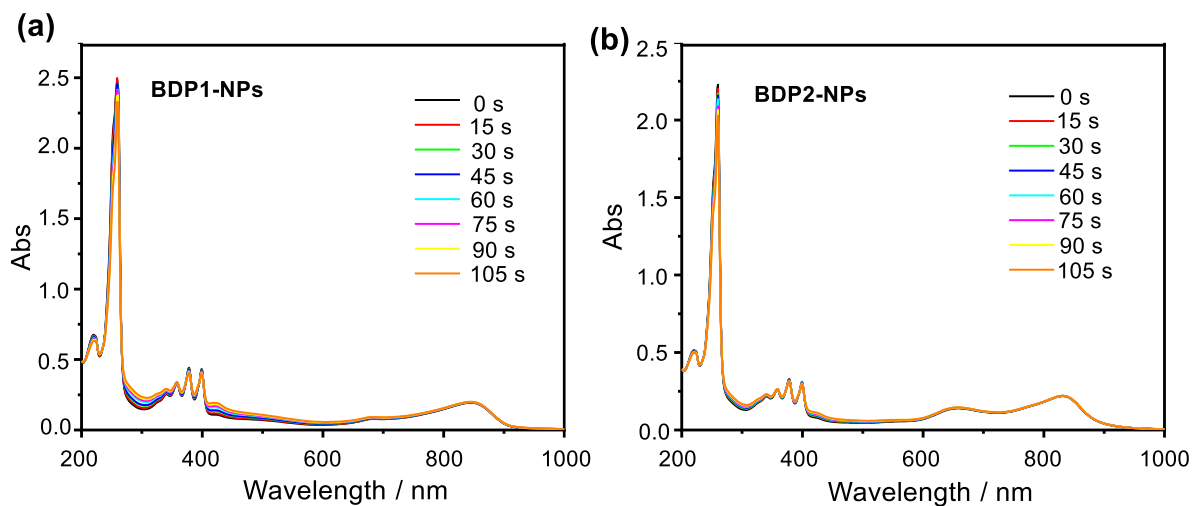


Figure S8. The consumption of ABDA in its mixtures with (a) **BDP1-NPs** and (b) **BDP2-NPs** under laser irradiation (808 nm, 0.96 W / cm²) at different time.

I.8 General animals culture

Animal experiments

All animal experiments were conducted in accordance with the approved agreement by the Institutional Animal Ethics Committee of China Pharmaceutical University (Approval Code: 2022-12-021). Furthermore, all laboratory animal procedures strictly adhered to the guidelines outlined in the National Institutes of Health Guide for the Care and Use of Laboratory Animals. Male C57BL/6 mice aged 3-4 weeks were sourced from the Comparative Medicine Centre at Yangzhou University, Yangzhou, China, and housed in a SPF-class laboratory facility. Each C57BL/6 mouse was subcutaneously injected with $1 \times 10^6/100 \mu\text{L}$ of Hepa1-6 cells to establish the Hepa1-6 tumor-bearing mouse model.

Phototoxicity and biocompatibility

Phototoxicity and biocompatibility tests were conducted using the classical MTT assay. HepG2 and Hepa1-6 cells (1×10^4 cells/well) were seeded into a 96-well plate with 150 μL of DMEM per well and cultured overnight in a 37°C incubator. Subsequently, 150 μL of DMEM containing **BDP2-NPs** at different concentrations (0, 10, 20, 30, 50, 100 μM) was added to the wells and incubated for 2 hours. For the phototoxicity group, an 808 nm laser (0.1 W/cm^2) was applied for 10 minutes, while the dark toxicity group received no laser treatment. The cells were then incubated for an additional 24 hours. Afterwards, the cells were washed three times with PBS and treated with 150 μL of MTT solution (0.5 mg/mL) for 4 hours. The MTT solution was carefully discarded in a lightproof environment, and 200 μL of DMSO was added to each well. The plate was shaken for 3 minutes, and the optical density (OD) was measured at a wavelength of 490 nm using a microplate reader.

Fluorescence microscopy apoptosis cell Imaging

Photodynamic-induced apoptosis was evaluated using the Calcein AM/PI apoptosis assay. Hepa1-6 cells (2×10^4 cells/well) were seeded into a 24-well plate and treated with **BDP2-NPs** at a concentration of 20 μM . Subsequently, the cells were continuously irradiated with an 808 nm laser (0.2 W/cm^2) for 0, 2, 4, 8 minutes. After a 4-hour incubation, the cells were washed three times with PBS. Calcein AM (5 μM) and PI (10 μM) were added to the wells, followed by an incubation at 37°C for 30 minutes. Subsequently, the cells were imaged using a fluorescence microscope. Calcein AM fluorescence was excited at 475/30 nm and collected at 530/40 nm, while PI fluorescence was excited at 540 nm and collected at 605/55 nm.

Detection of cell apoptosis by flow cytometry

Hepa1-6 cells (2×10^5 /well) were seeded into 6-well plate and added **BDP2-NPs** of 20 μM . After 2h, continuously irradiated with 808nm laser (0.1 W/cm^2) for 0, 2, 4, 8 minutes. 4h later, Annexin V-FITC/PI Apoptosis Detection Kit was used to evaluate cell apoptosis.

PA imaging in vivo

For PA imaging of tumor *in vivo*, Hepa1-6 tumor-bearing C57BL/6 mice (n=3 for each group) were administered **BDP2-NPs** (100 μM , 100 μL) via tail vein. The imaging was performed at 0, 6, 12, 36, and 60 hours post-administration. Additional acquisition parameters are as follows: Frequency: 21MHz, PA Gain: 45dB, B-Mode Gain: 18dB, Persistence: 6, Acquisition Wavelength: 820 nm.

Statistical analysis

The results are shown as mean \pm standard deviation (SD) unless stated otherwise. For all tests, $P < 0.05$ was considered statistically significant.

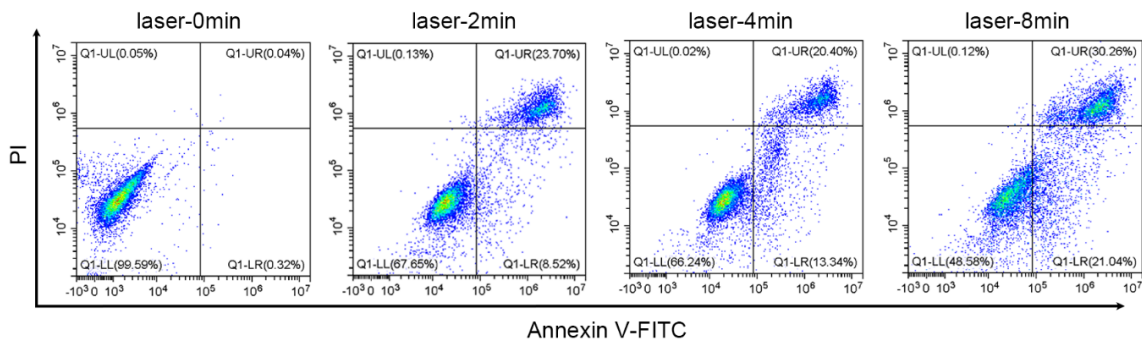


Figure S9. Photothermal-induced apoptosis was detected by flow cytometry.

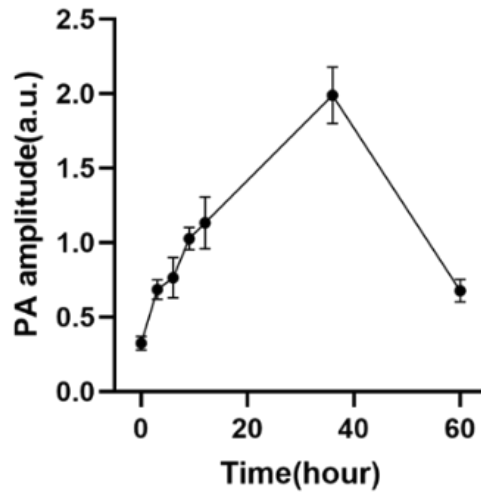


Figure S10. Changes of photoacoustic intensity at tumor site in mice (n=3) after injection of **BDP2-NPs** (100 μ M, 100 μ L)

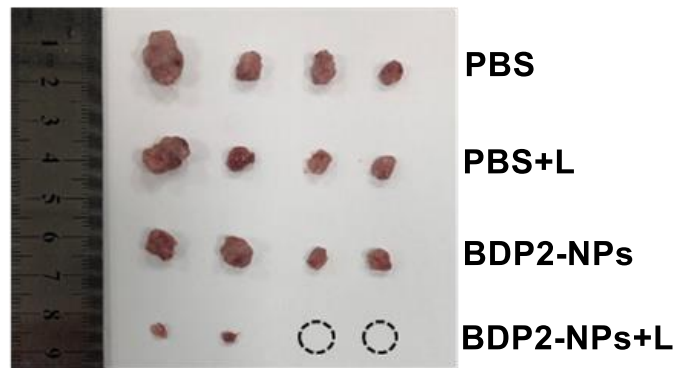


Figure S11. Tumor tissue images of tumor-bearing mice after 15 days of different treatments .

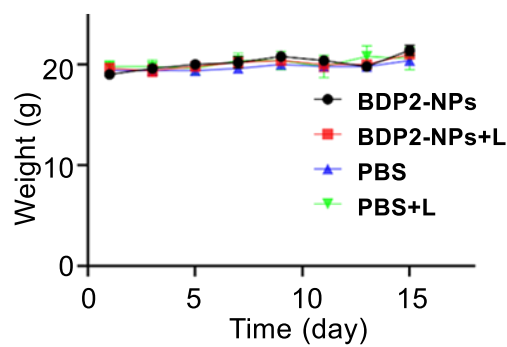


Figure S12. Body weight changes of tumor-bearing mice during different treatments (n=3).

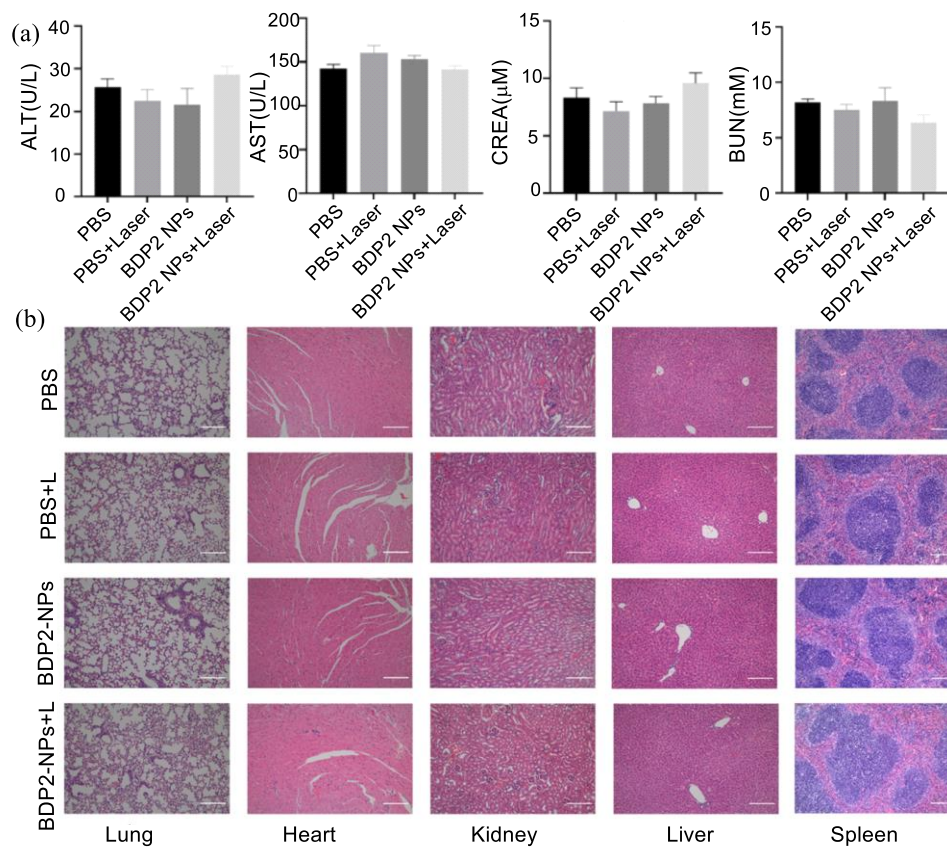
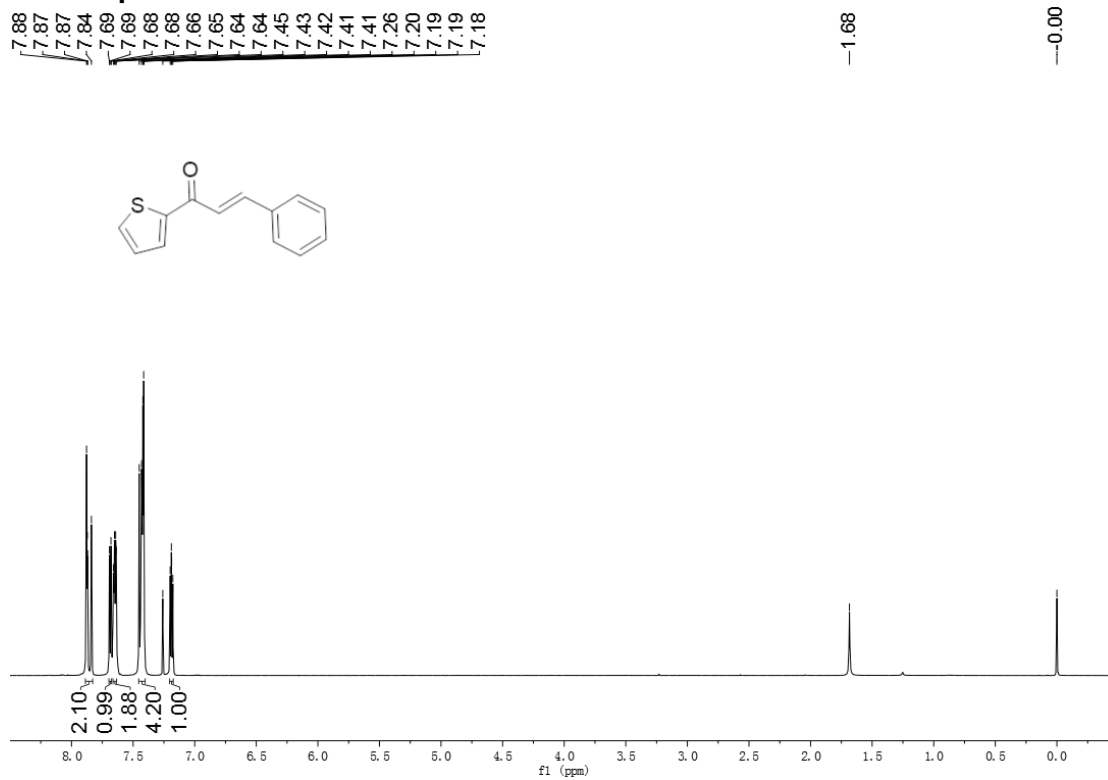
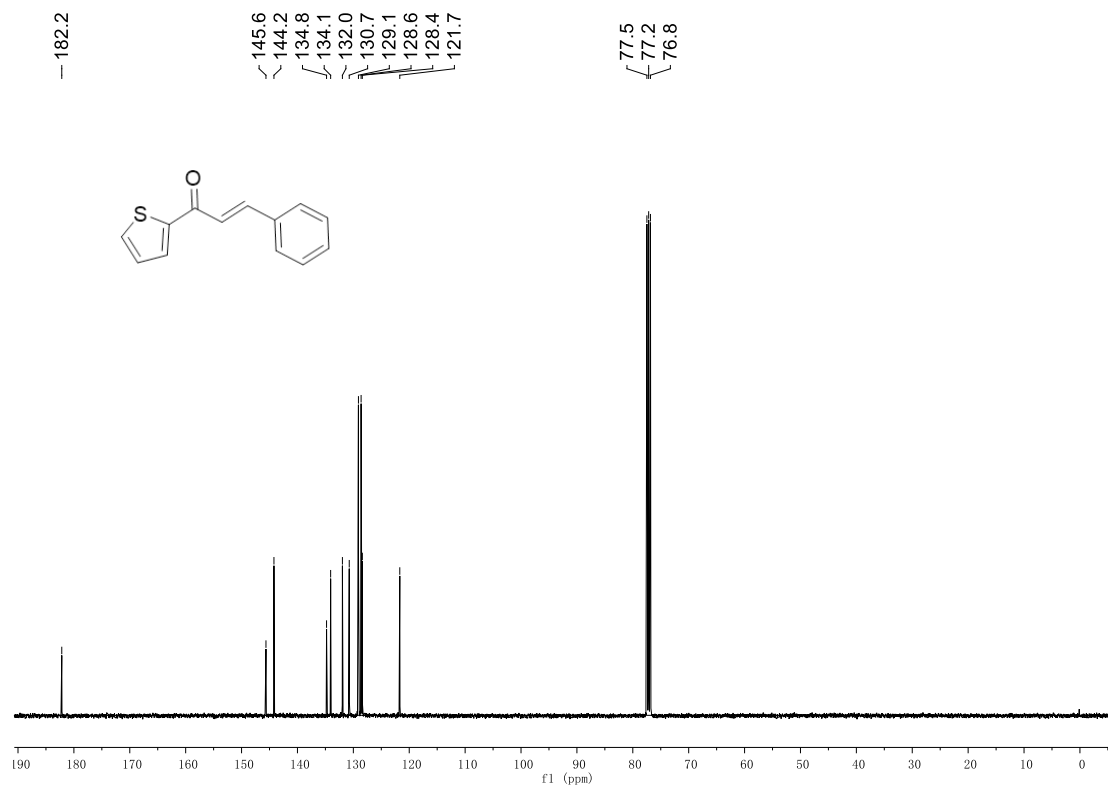


Figure S13. (a) Investigation of ALT, AST, CREA, and BUN in the blood of different groups of mice in overall biocompatibility evaluation (n=3) (b) H&E staining (20x) of mice heart, liver, spleen, lung and kidney in different groups in the overall biocompatibility evaluation

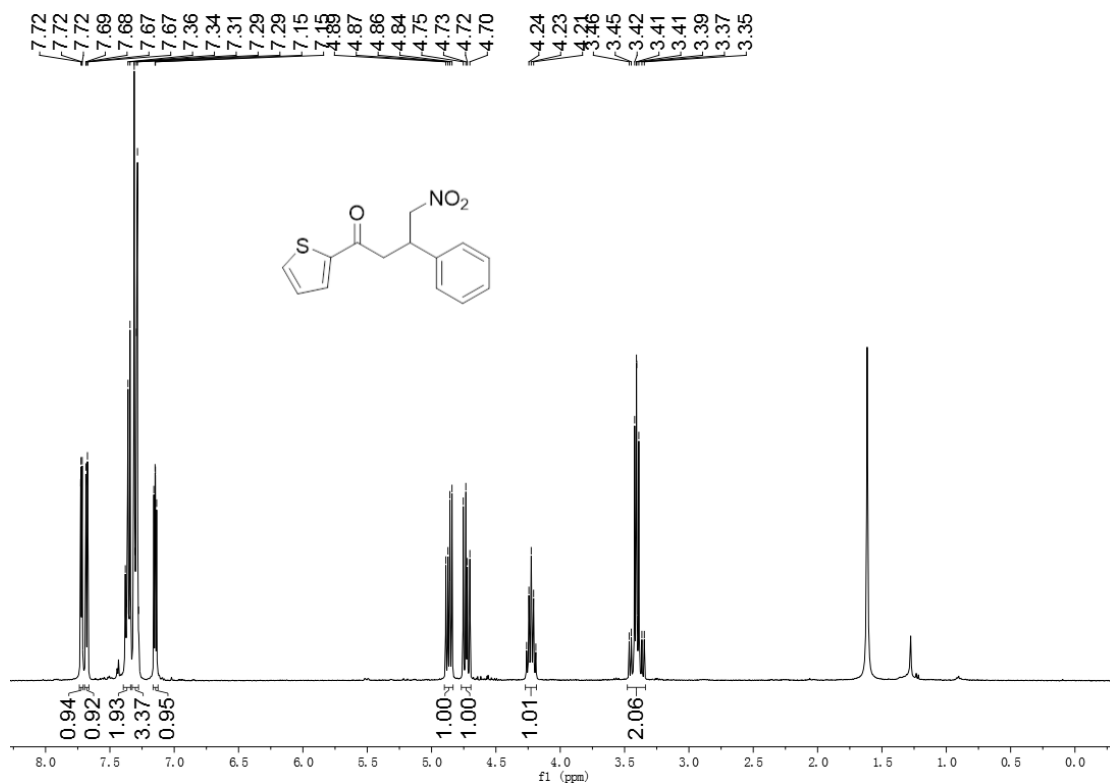
II. ^1H , ^{13}C NMR spectra and HRMS-ESI



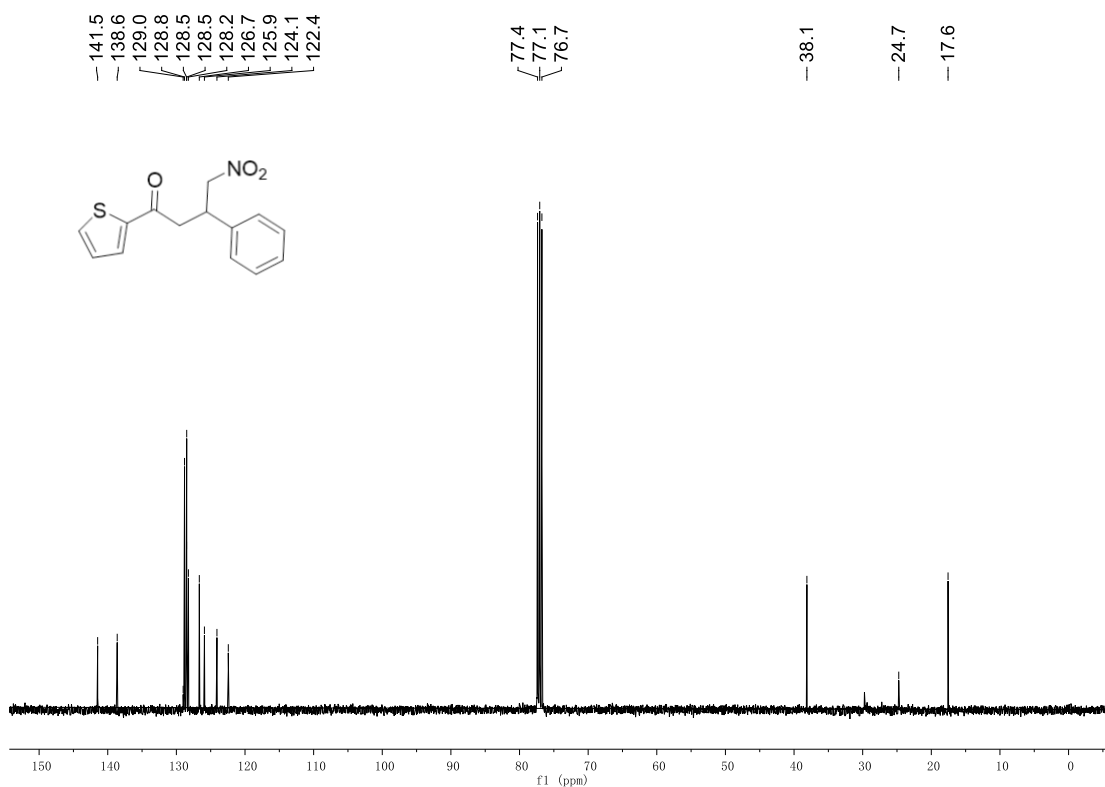
1a ^1H NMR (400MHz, CDCl_3)



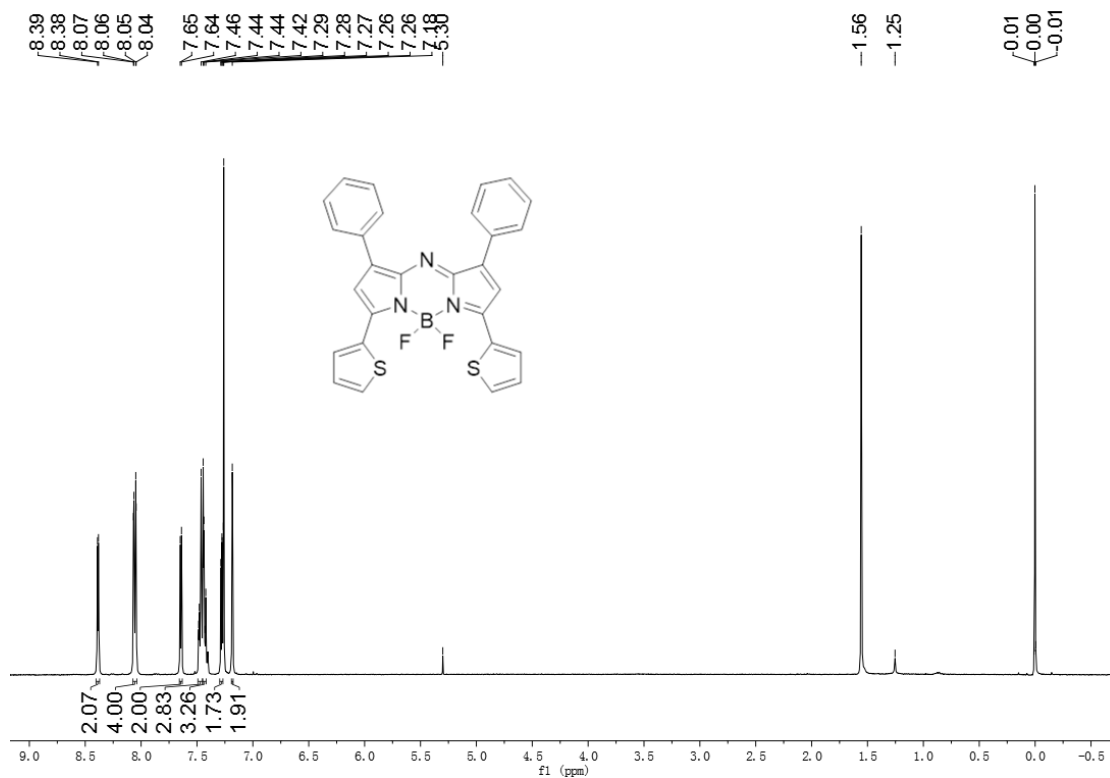
1a ^{13}C NMR (101MHz, CDCl_3)



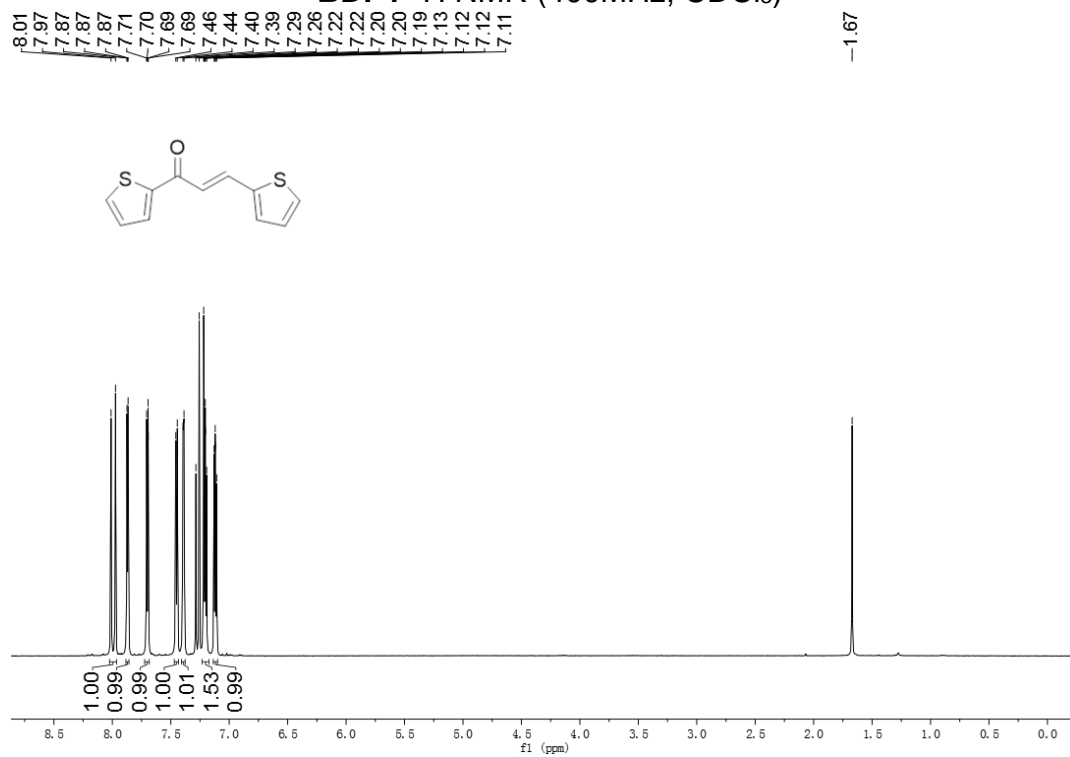
2a ¹H NMR (400MHz, CDCl₃)



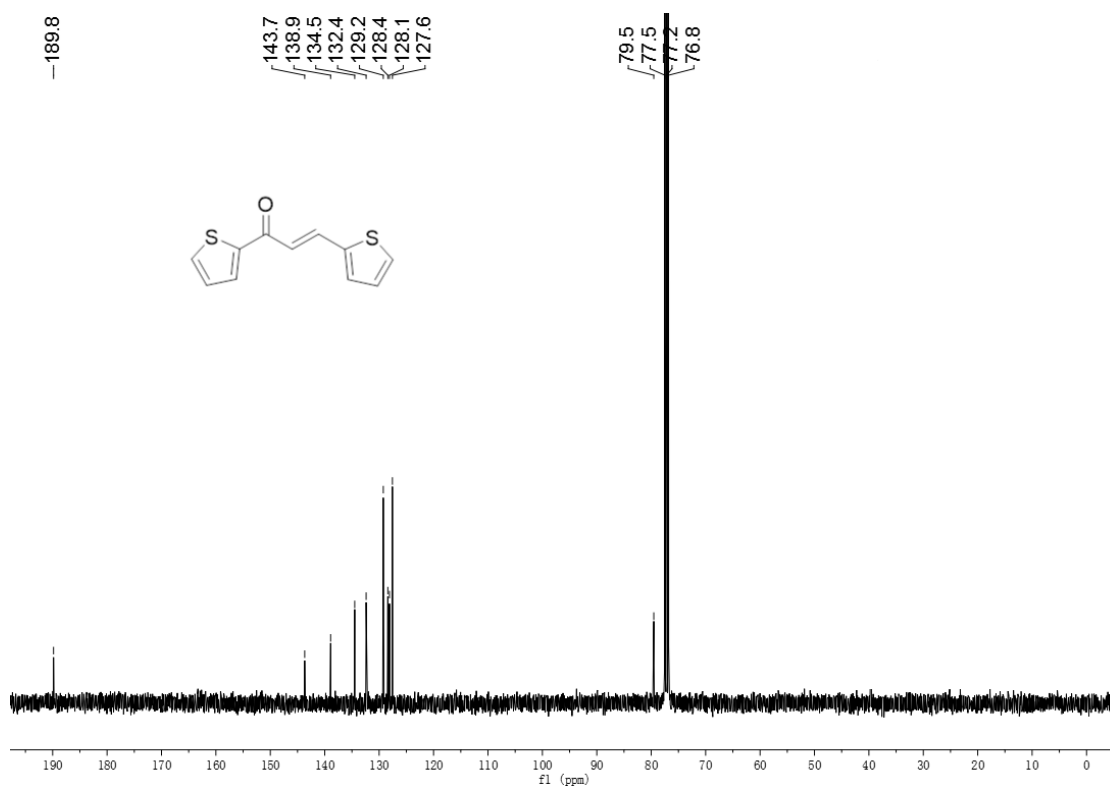
2a ¹³C NMR (101MHz, CDCl₃)



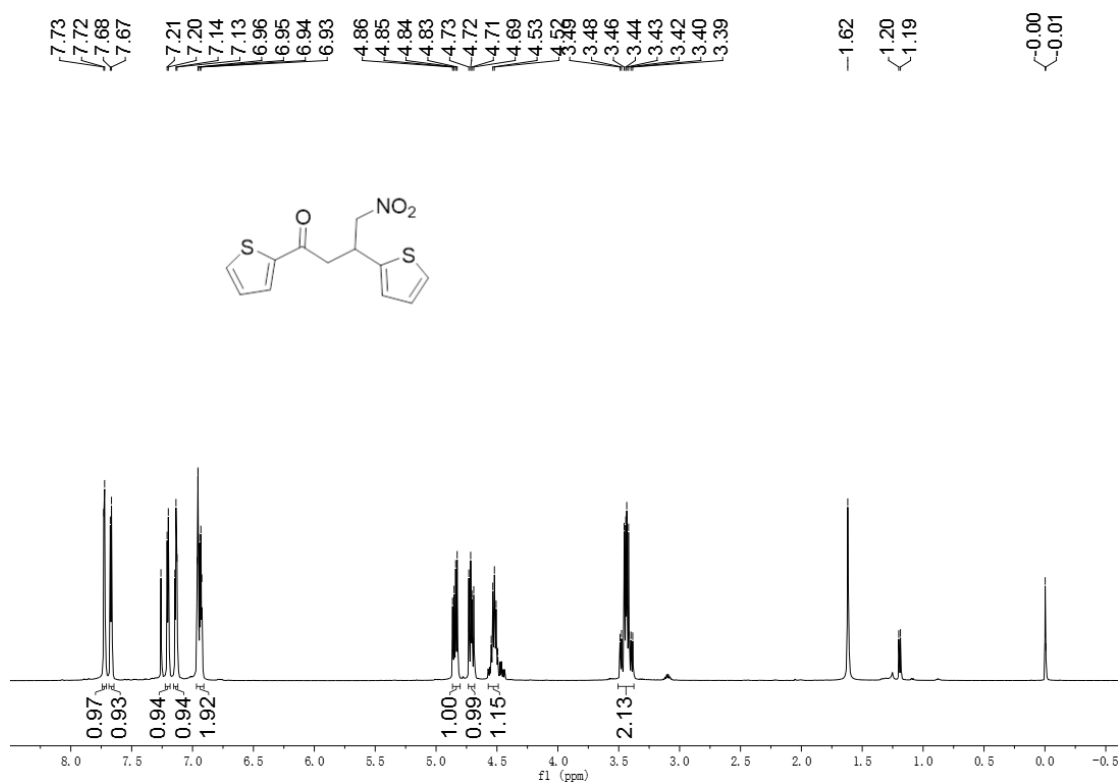
BDP1 ^1H NMR (400MHz, CDCl_3)



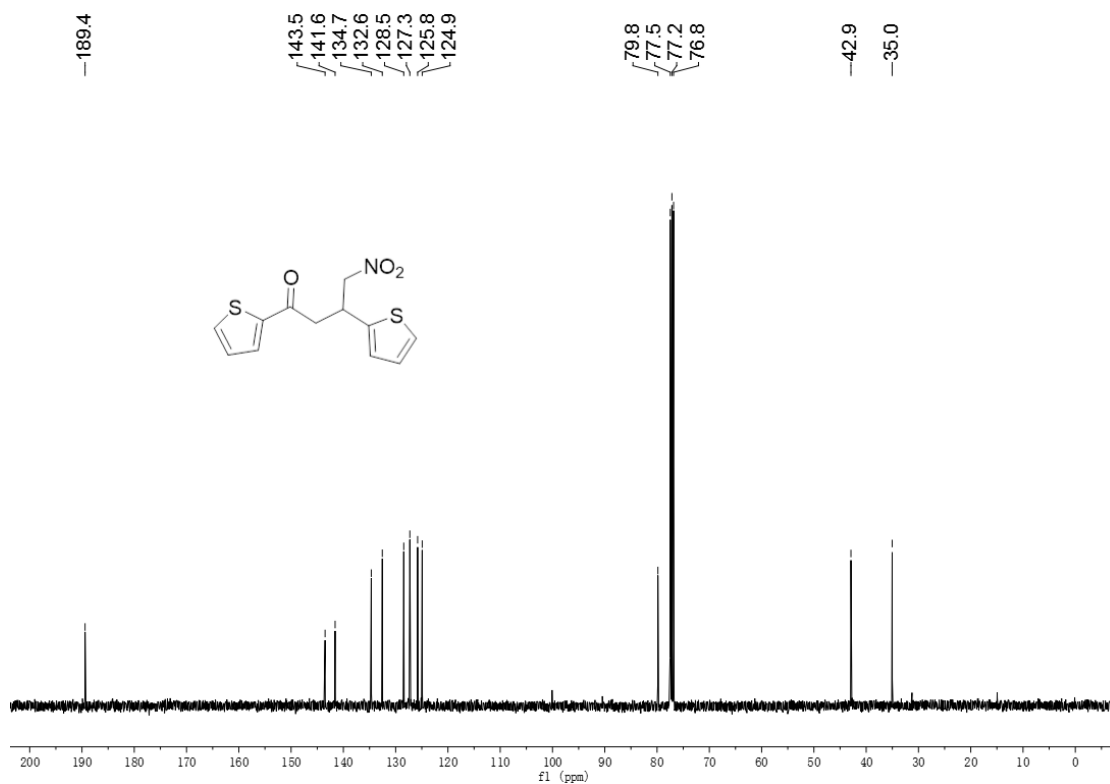
1b ^1H NMR (400MHz, CDCl_3)



1b ^{13}C NMR (101MHz, CDCl_3)



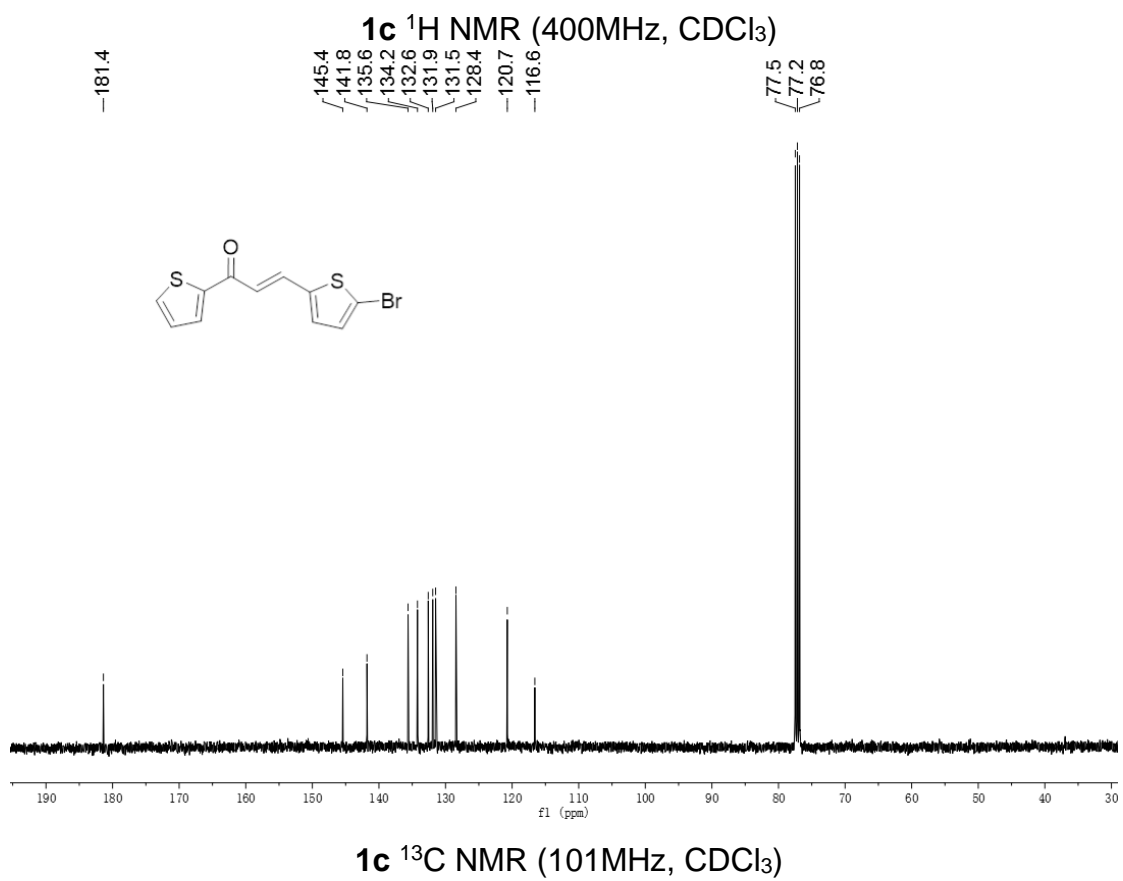
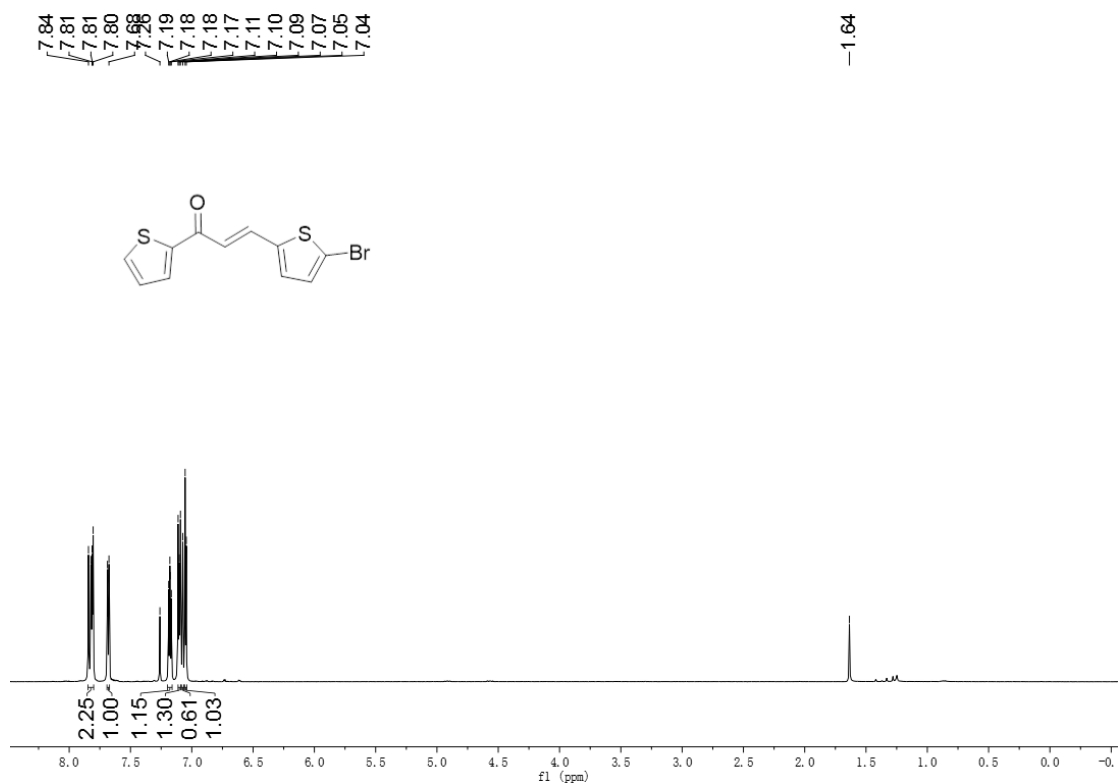
2b ^1H NMR (400MHz, CDCl_3)

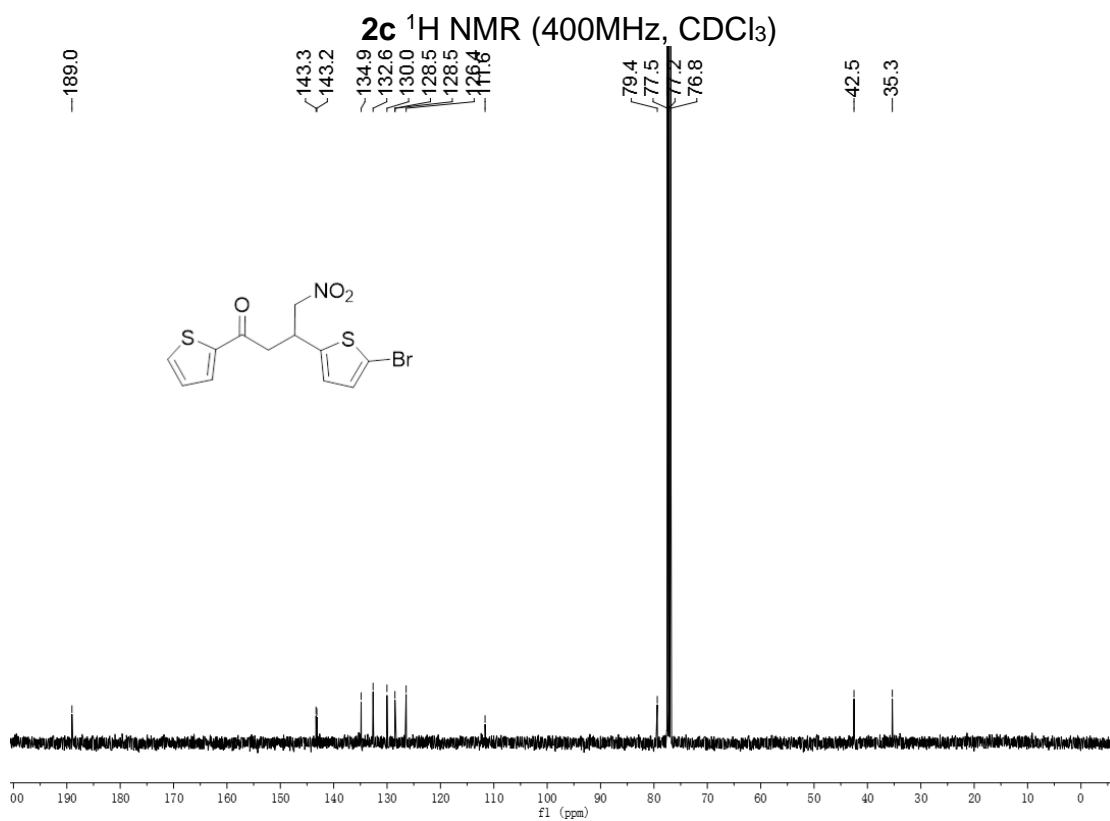
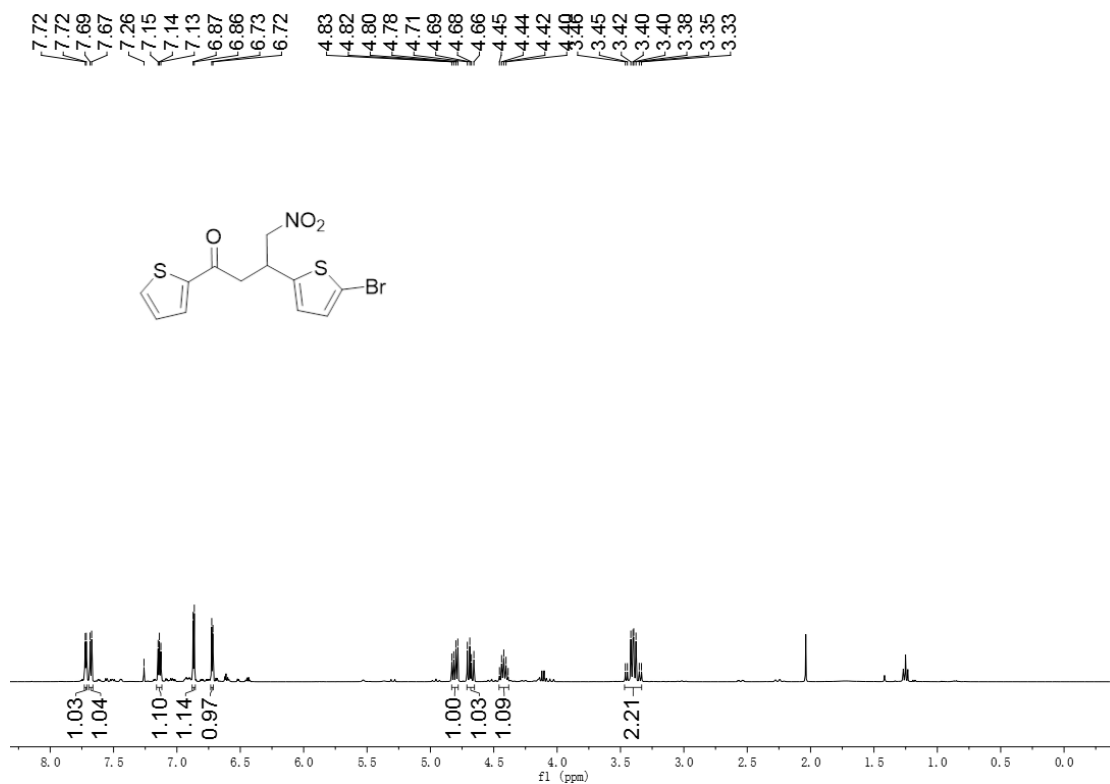


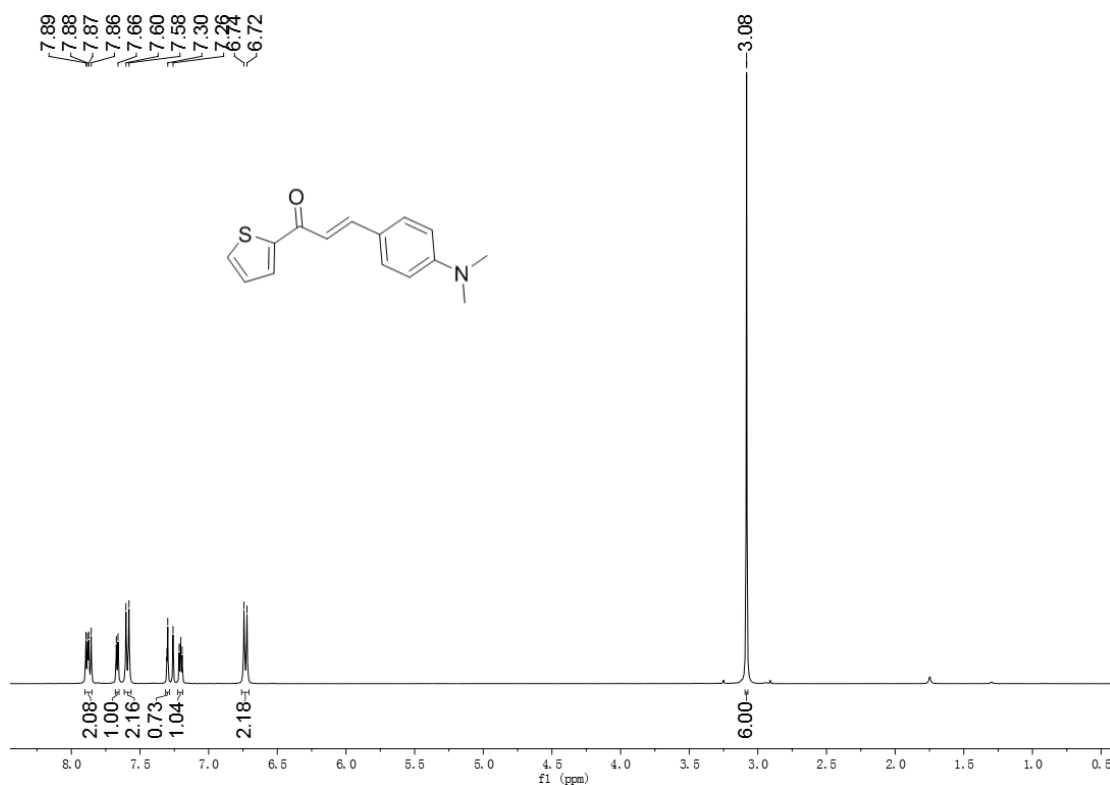
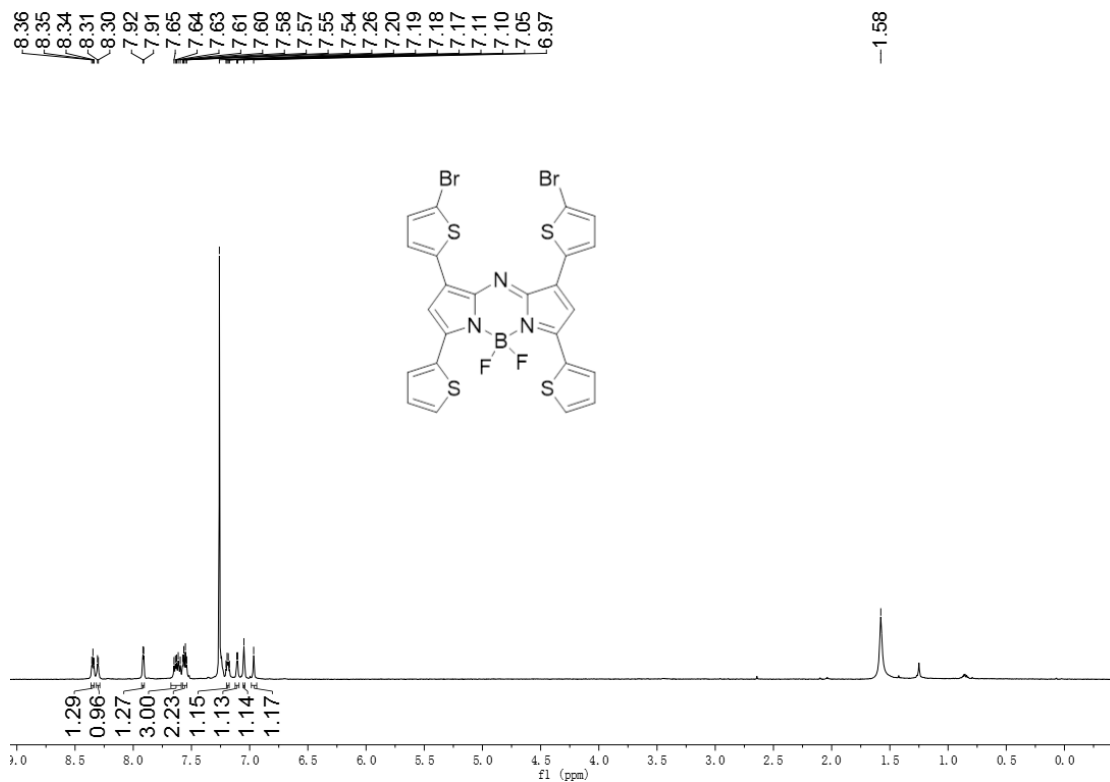
2b ^{13}C NMR (101MHz, CDCl_3)

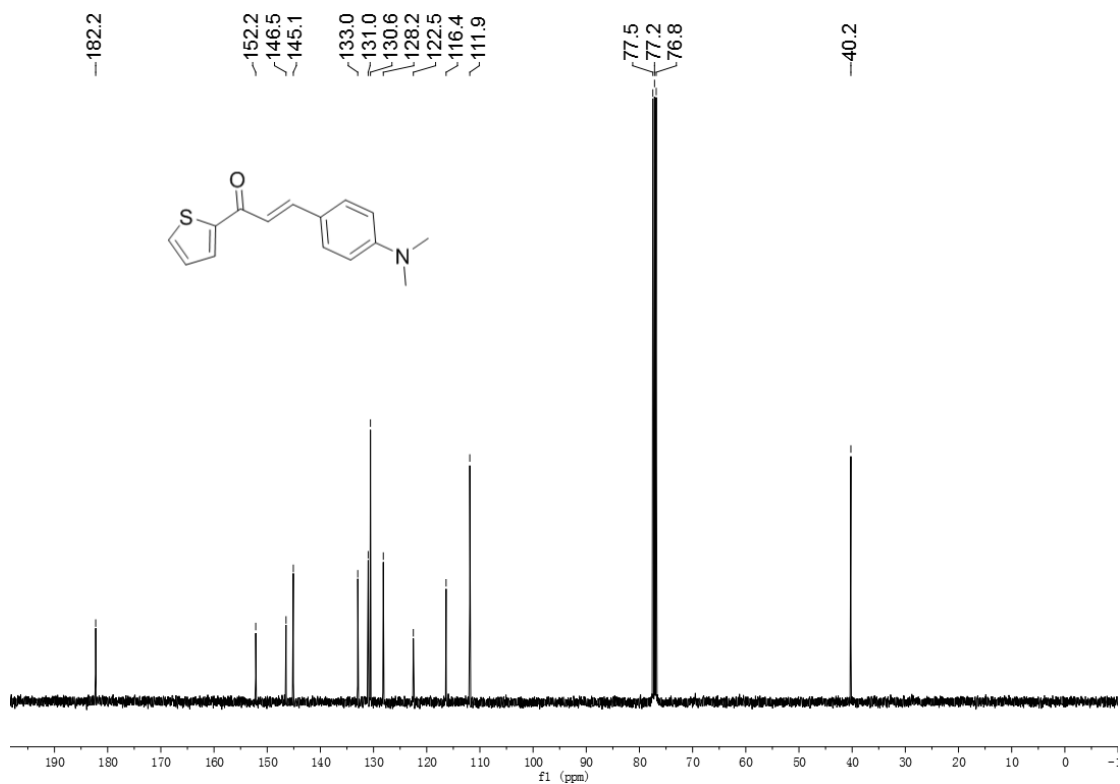


BDP2 ^1H NMR (400MHz, CDCl_3)

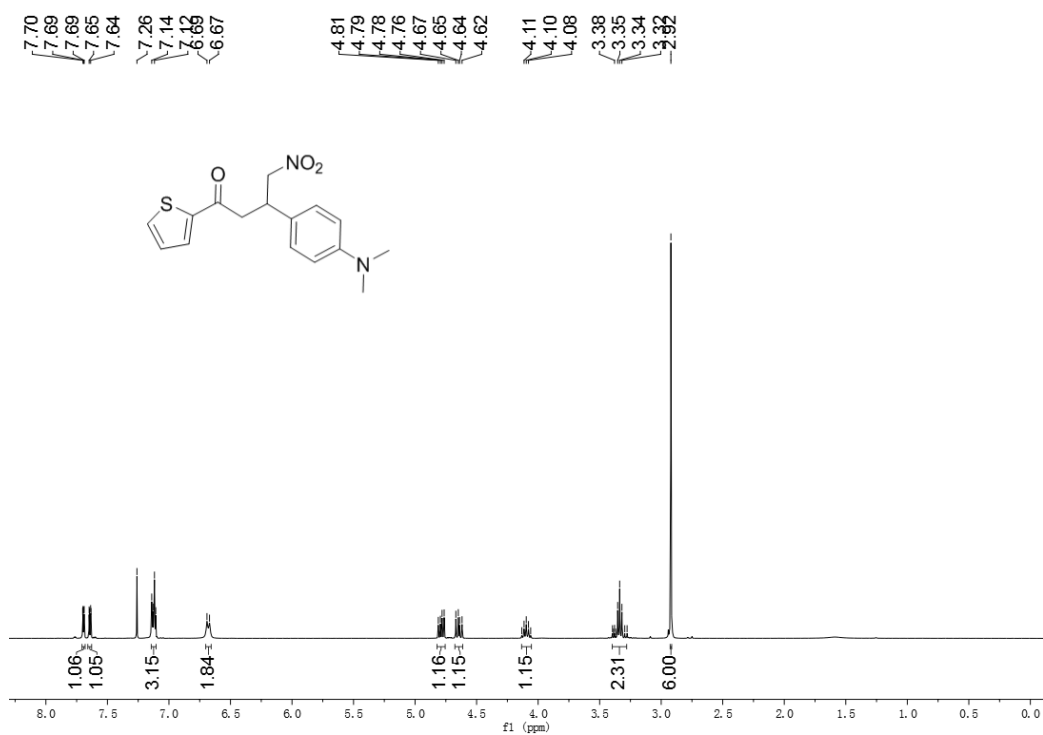




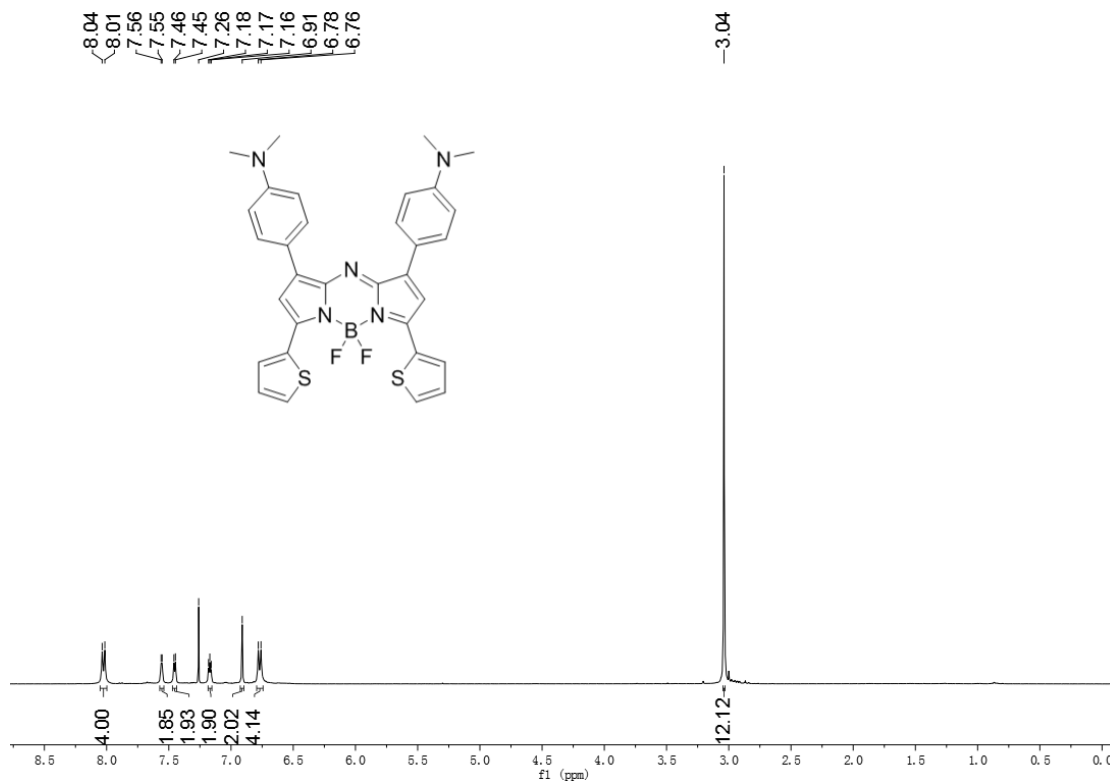
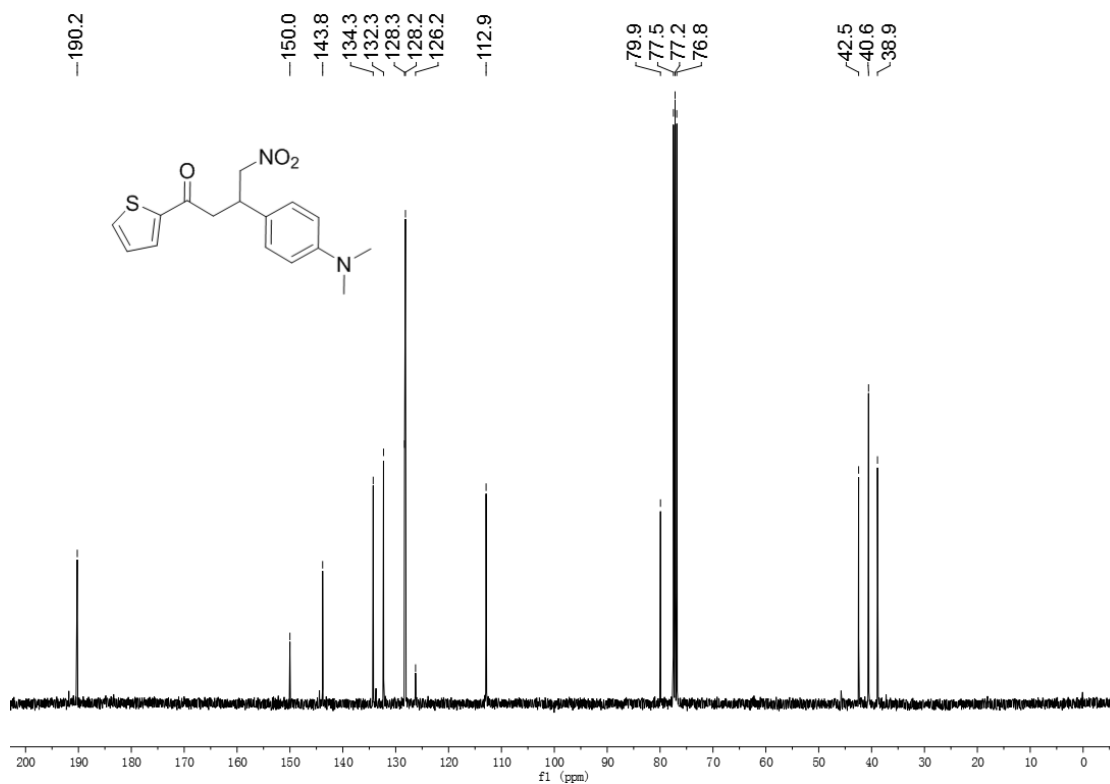


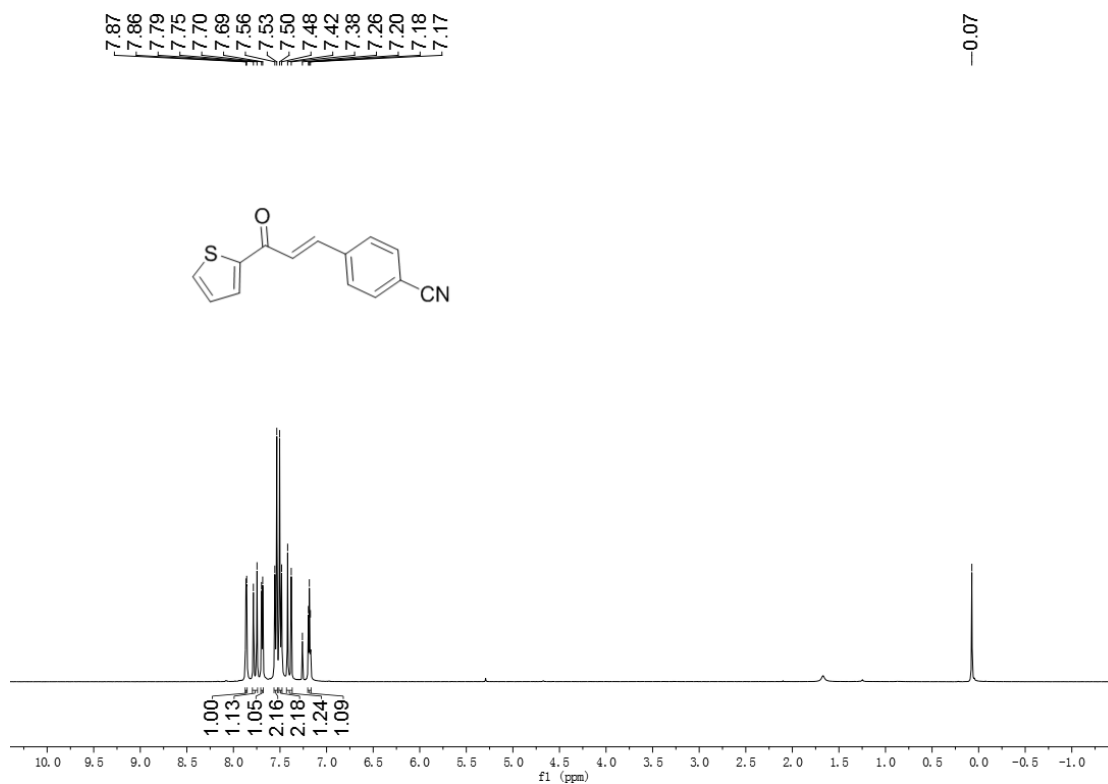


1d ^{13}C NMR (101MHz, CDCl_3)

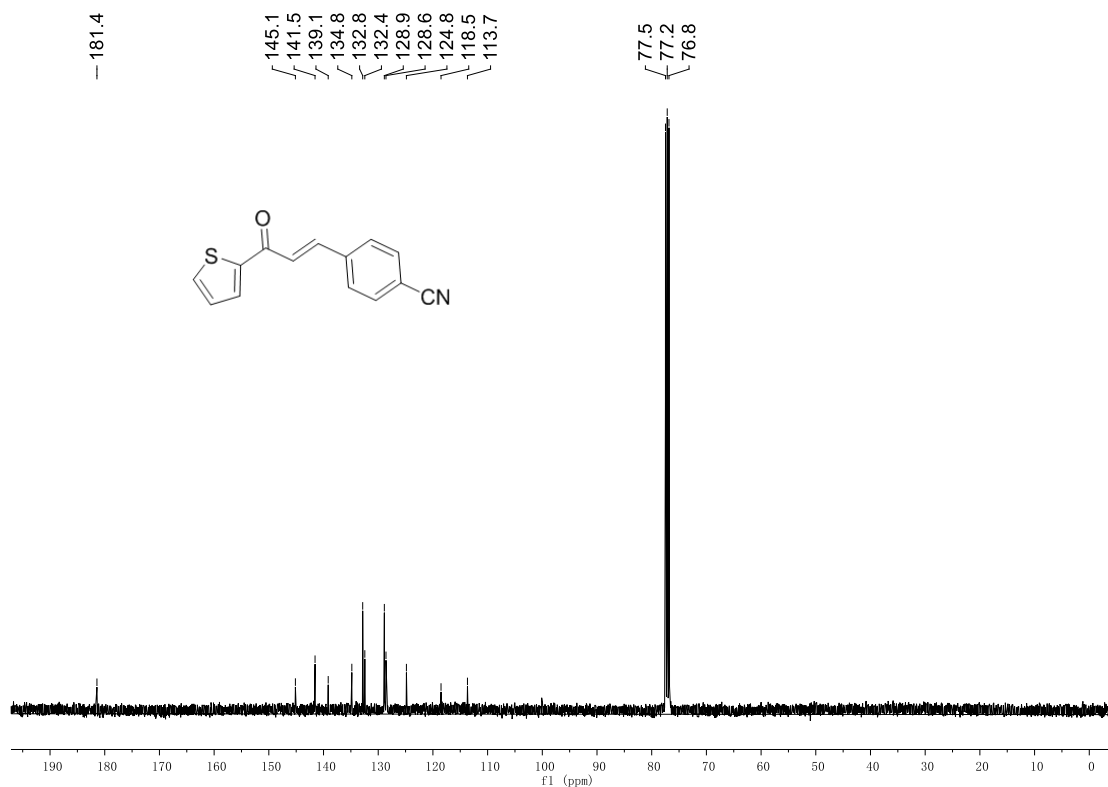


2d ^1H NMR (400MHz, CDCl_3)

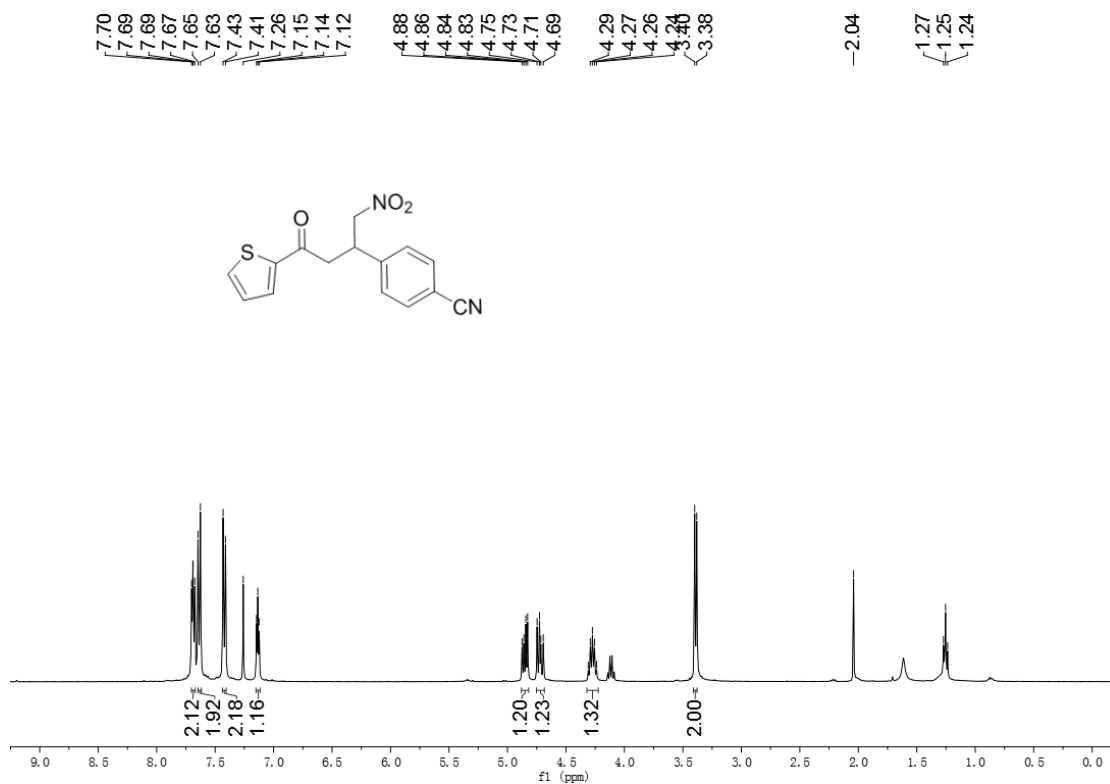




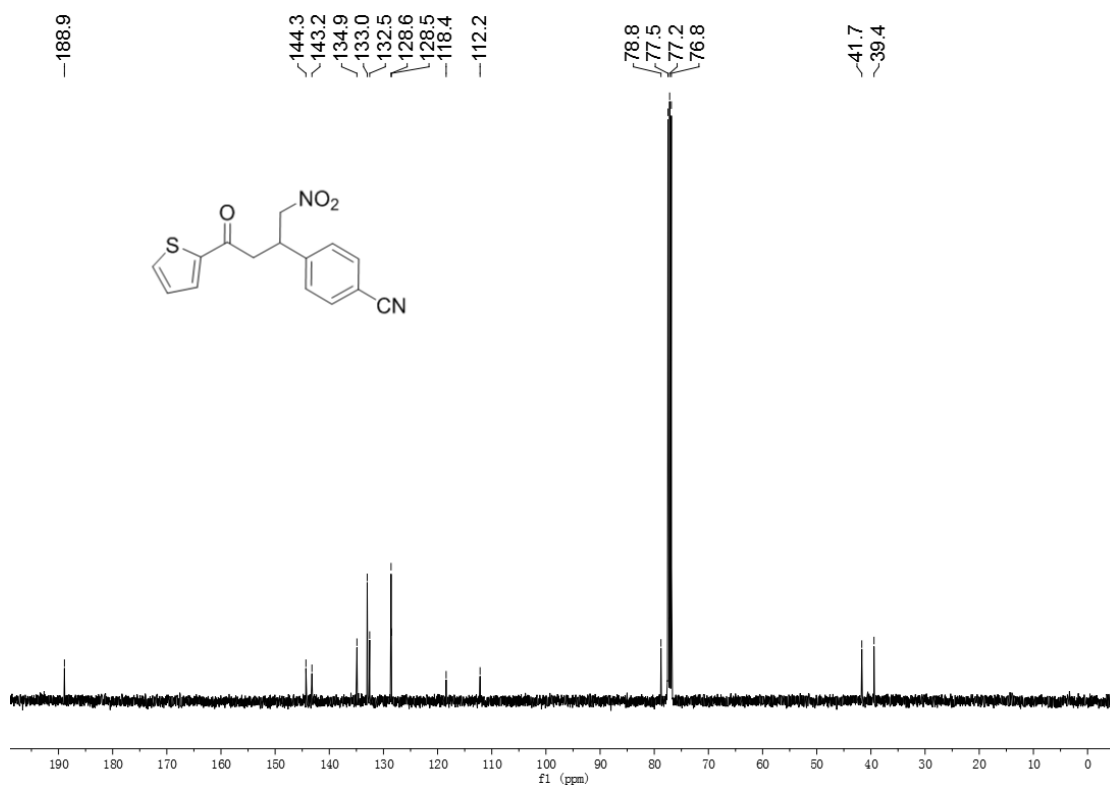
1e ^1H NMR (400MHz, CDCl_3)



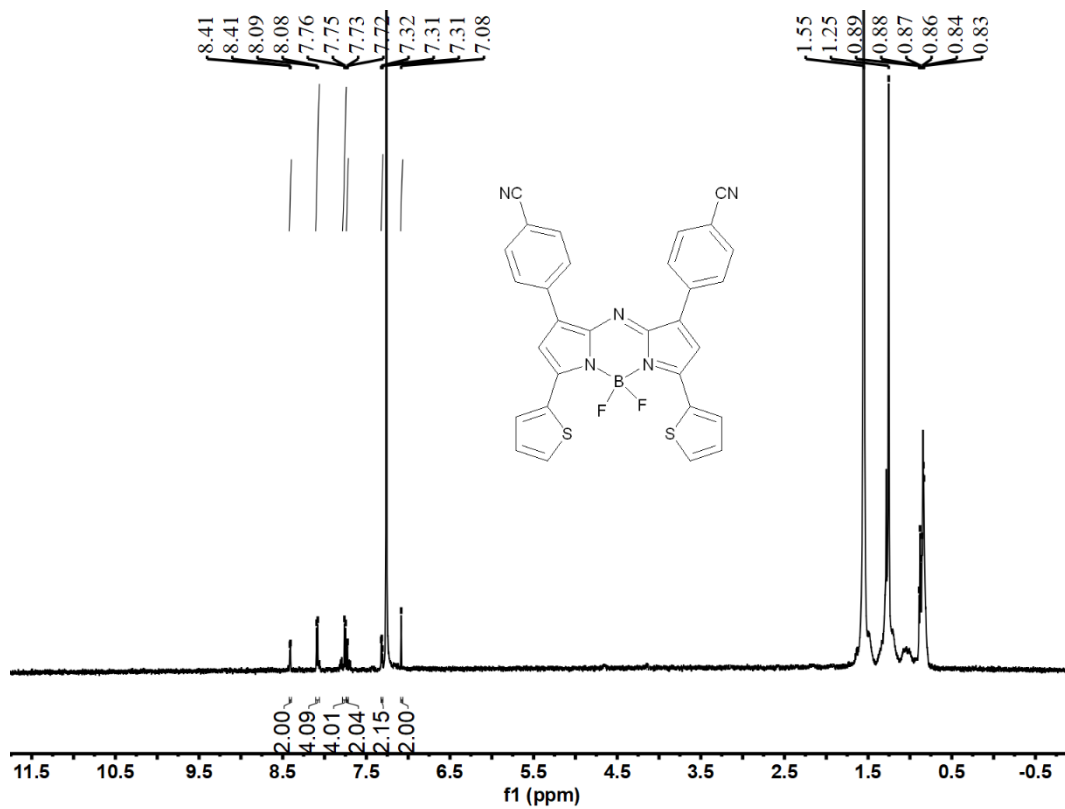
1e ^{13}C NMR (101MHz, CDCl_3)



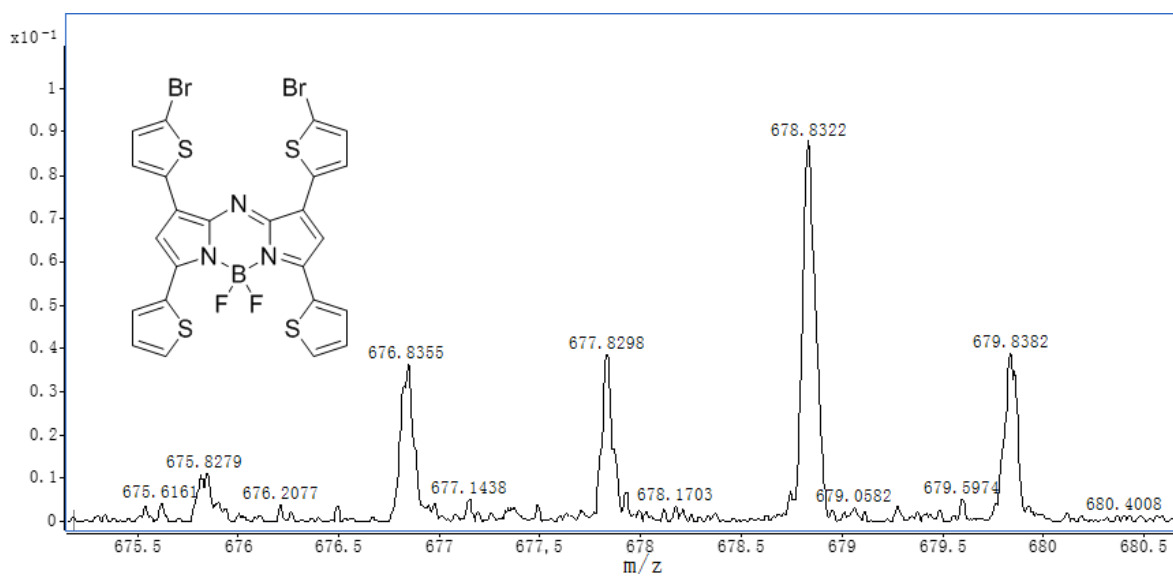
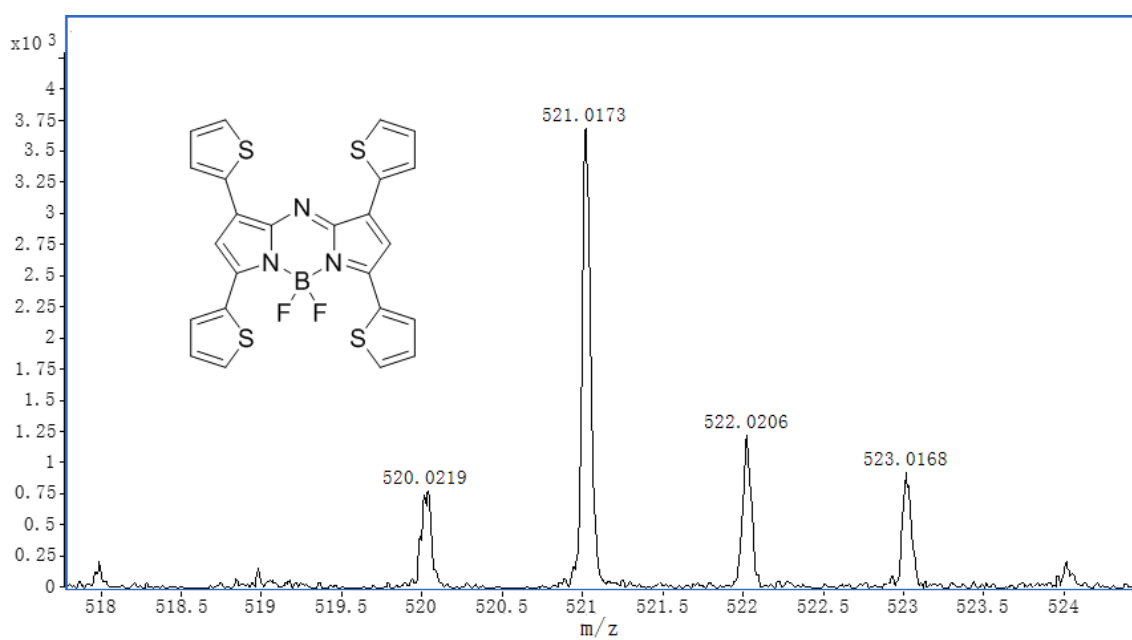
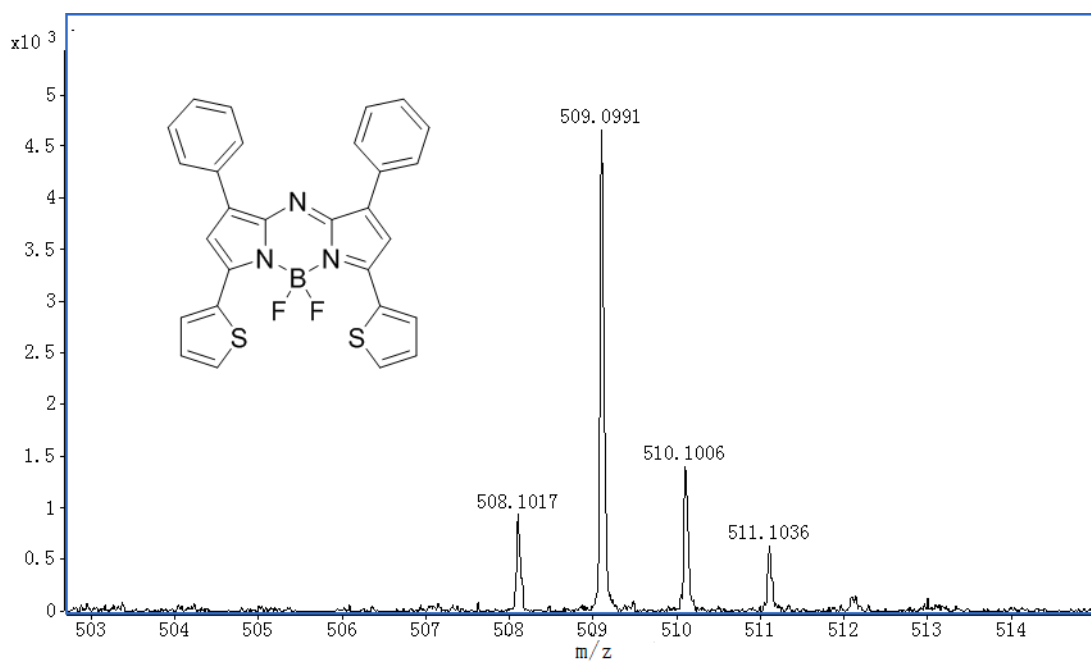
2e ^1H NMR (400MHz, CDCl_3)

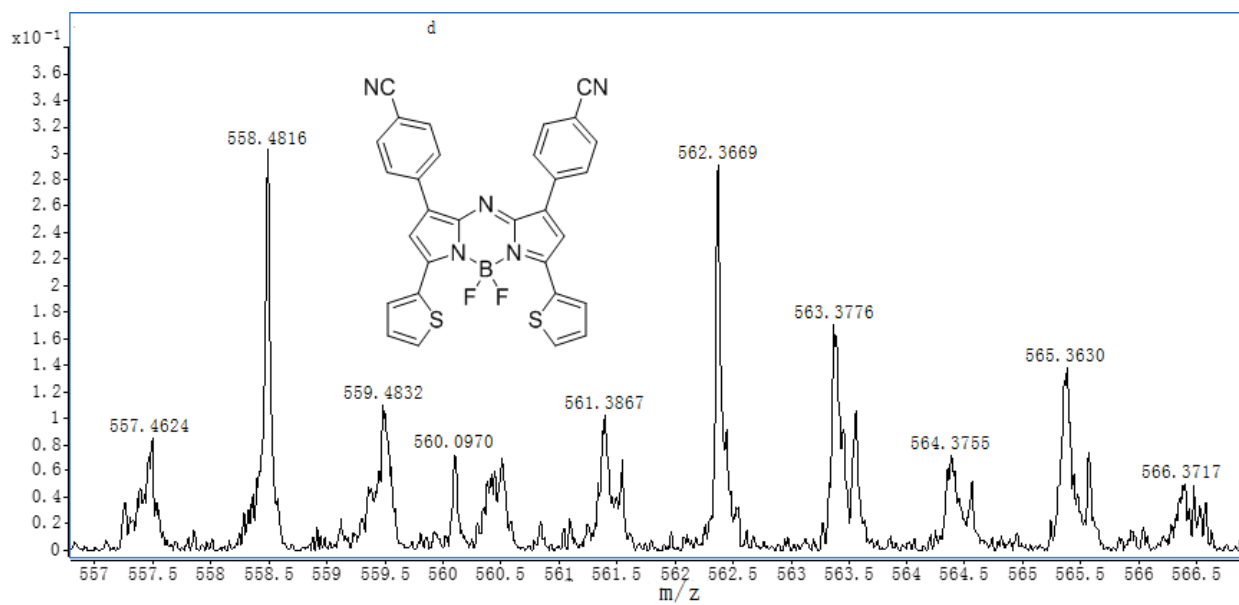
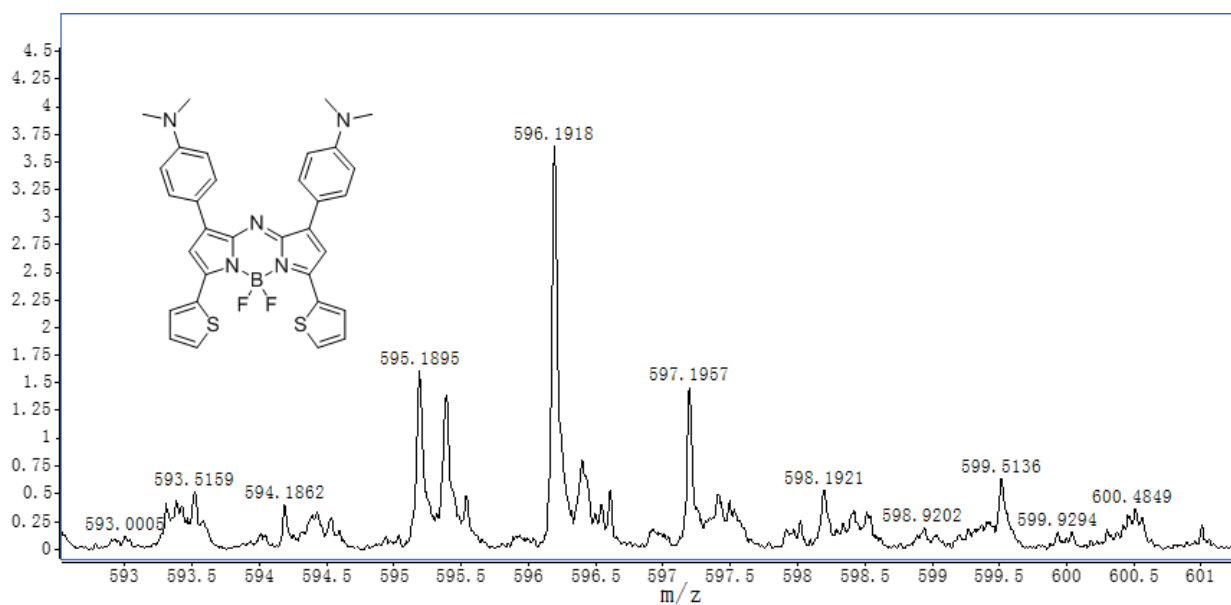


2e ^{13}C NMR (101MHz, CDCl_3)



BDP5 ^1H NMR (400MHz, CDCl_3)





III Cartesian coordinates

DFT optimized S0 state geometry of **BDP1**.

Center Number	Atomic Number	Atomic Type	Coordinates (Angstroms)		
			X	Y	Z
1	16	0	-4.797643	-2.574519	-0.583924
2	16	0	4.763479	-2.639254	-0.548234
3	1	0	1.617040	-3.685012	0.930592
4	1	0	-1.666794	-3.665913	0.895086
5	9	0	-0.028733	-2.418207	1.345194
6	9	0	-0.000933	-2.533111	-0.944532
7	7	0	0.010865	1.305212	0.104413
8	7	0	1.247788	-0.750938	0.136570
9	7	0	-1.254102	-0.734309	0.103878
10	6	0	-4.758974	-4.266597	-0.242371
11	1	0	-5.617398	-4.882107	-0.473298
12	6	0	-3.560953	-4.649959	0.303468
13	1	0	-3.338432	-5.670456	0.592265
14	6	0	-3.155797	-2.362860	0.023332
15	6	0	-2.584141	-1.037576	0.032895
16	6	0	-3.331083	0.167660	-0.043871
17	1	0	-4.408029	0.215186	-0.114029
18	6	0	-2.453226	1.240532	-0.021398
19	6	0	-1.139710	0.654866	0.069291
20	6	0	-2.796959	2.665302	-0.061889
21	6	0	-4.062245	3.090016	0.388234
22	1	0	-4.753096	2.362918	0.803593
23	6	0	-4.426640	4.432017	0.337804
24	1	0	-5.405209	4.737530	0.696445
25	6	0	-3.534631	5.382665	-0.163495
26	1	0	-3.818391	6.430205	-0.203713
27	6	0	-2.275993	4.976823	-0.610558
28	1	0	-1.577245	5.708375	-1.005872
29	6	0	-1.906611	3.634479	-0.563008
30	1	0	-0.930081	3.326294	-0.914249
31	6	0	4.699595	-4.331246	-0.209442
32	1	0	5.548453	-4.959369	-0.441725
33	6	0	3.496214	-4.697402	0.336611
34	1	0	3.258767	-5.714907	0.624086

35	6	0	3.126245	-2.404256	0.061091
36	6	0	2.574450	-1.070845	0.074580
37	6	0	3.339345	0.124753	0.038101
38	1	0	4.419101	0.158274	0.042385
39	6	0	2.475467	1.208476	0.093385
40	6	0	1.153011	0.639400	0.140014
41	6	0	2.833694	2.629159	0.096133
42	6	0	2.005625	3.604499	0.684377
43	1	0	1.068476	3.303034	1.135231
44	6	0	2.386027	4.944569	0.691354
45	1	0	1.736414	5.681472	1.154629
46	6	0	3.595417	5.340976	0.117608
47	1	0	3.888799	6.386582	0.126939
48	6	0	4.425894	4.383798	-0.469929
49	1	0	5.365031	4.682628	-0.926279
50	6	0	4.049540	3.044225	-0.480933
51	1	0	4.689336	2.311029	-0.962255
52	5	0	-0.009394	-1.688114	0.144627
53	6	0	2.600999	-3.608946	0.491468
54	6	0	-2.649225	-3.574981	0.455745

SCF done: -2263.198411 Hartree

No imaginary Frequency.

DFT optimized S0 state geometry of **BDP2**.

Center Number	Atomic Number	Atomic Type	Coordinates (Angstroms)		
			X	Y	Z
1	16	0	4.560592	-3.001807	-0.477290
2	16	0	0.122902	5.413046	-0.707345
3	1	0	2.491926	3.172131	0.887718
4	1	0	3.992670	0.253837	1.024709
5	9	0	2.118476	1.140048	1.367941
6	9	0	2.271271	1.162676	-0.919254
7	7	0	-1.156599	-0.612056	0.092964
8	7	0	0.081709	1.445993	0.096206
9	7	0	1.241146	-0.761858	0.144392

10	6	0	6.021834	-2.169057	-0.085017
11	1	0	6.977100	-2.629517	-0.295974
12	6	0	5.775160	-0.939575	0.469081
13	1	0	6.559216	-0.262563	0.787317
14	6	0	3.578814	-1.665277	0.120594
15	6	0	2.140399	-1.792472	0.094032
16	6	0	1.439993	-3.017493	-0.000258
17	1	0	1.907465	-3.989546	-0.053036
18	6	0	0.075038	-2.749506	-0.005369
19	6	0	-0.035637	-1.315358	0.087774
20	6	0	1.643421	6.158975	-0.368931
21	1	0	1.806468	7.194226	-0.634860
22	6	0	2.519825	5.285308	0.221306
23	1	0	3.525958	5.560208	0.515416
24	6	0	0.669459	3.878072	-0.035638
25	6	0	-0.254789	2.769057	0.003377
26	6	0	-1.663764	2.889695	-0.035566
27	1	0	-2.199842	3.827055	-0.049599
28	6	0	-2.219485	1.617032	0.044538
29	6	0	-1.100666	0.710674	0.106043
30	5	0	1.498454	0.782530	0.157464
31	6	0	1.972550	3.990963	0.411827
32	6	0	4.392067	-0.649393	0.587276
33	6	0	-0.985810	-3.724835	-0.091438
34	6	0	-3.116695	-4.981036	-0.429386
35	6	0	-2.065270	-5.807323	-0.124603
36	1	0	-4.145491	-5.254673	-0.619673
37	1	0	-2.153356	-6.883761	-0.035655
38	6	0	-3.628425	1.303304	0.074860
39	6	0	-5.893434	0.318314	0.440277
40	6	0	-5.950825	1.578614	-0.098301
41	1	0	-6.715961	-0.337210	0.691537
42	1	0	-6.877318	2.084414	-0.343621
43	6	0	-0.855122	-5.094471	0.064058
44	6	0	-4.665177	2.139662	-0.301452
45	1	0	-4.496761	3.121486	-0.728321
46	1	0	0.085702	-5.566312	0.322258
47	16	0	-2.647172	-3.317789	-0.477903
48	16	0	-4.266467	-0.208121	0.692340

SCF done: -2904.704136 Hartree

No imaginary Frequency.

DFT optimized S0 state geometry of **BDP3**.

Center Number	Atomic Number	Atomic Type	Coordinates (Angstroms)		
			X	Y	Z
1	16	0	-4.129698	4.737752	-0.266333
2	16	0	-3.955426	-4.750843	-0.909144
3	1	0	-5.052412	-1.756180	0.825568
4	1	0	-5.075982	1.514604	1.110541
5	9	0	-3.798293	-0.133848	1.372355
6	9	0	-3.960448	0.015864	-0.909454
7	7	0	-0.093522	0.013561	0.080629
8	7	0	-2.126205	-1.265729	0.037704
9	7	0	-2.167377	1.222441	0.196583
10	6	0	-5.806396	4.633755	0.133048
11	1	0	-6.454220	5.482142	-0.039088
12	6	0	-6.135202	3.402637	0.639168
13	1	0	-7.137762	3.137362	0.953449
14	6	0	-3.849556	3.079418	0.261632
15	6	0	-2.507972	2.548647	0.205030
16	6	0	-1.332429	3.331621	0.139444
17	1	0	-1.313993	4.411315	0.135517
18	6	0	-0.234160	2.478806	0.093664
19	6	0	-0.779373	1.145081	0.130696
20	6	0	-5.646585	-4.746940	-0.560296
21	1	0	-6.260023	-5.585410	-0.859836
22	6	0	-6.032349	-3.599252	0.083256
23	1	0	-7.052710	-3.405153	0.392229
24	6	0	-3.748124	-3.165021	-0.168638
25	6	0	-2.423441	-2.593530	-0.112345
26	6	0	-1.220792	-3.333530	-0.192424
27	1	0	-1.165660	-4.410135	-0.255642
28	6	0	-0.150914	-2.451352	-0.080734
29	6	0	-0.740212	-1.142027	0.043887
30	5	0	-3.092962	-0.040045	0.160152
31	6	0	-4.959915	-2.699110	0.306958

32	6	0	-5.029572	2.518058	0.713539
33	6	0	1.150881	2.872988	0.018330
34	6	0	3.612254	3.040630	-0.293010
35	6	0	3.054355	4.253815	0.014859
36	1	0	3.624152	5.168764	0.113646
37	6	0	1.247279	-2.805290	-0.075785
38	6	0	3.708685	-2.955043	0.247474
39	6	0	3.196062	-4.099917	-0.304724
40	1	0	3.798826	-4.958331	-0.571872
41	6	0	1.652042	4.152205	0.188123
42	6	0	1.793179	-4.010233	-0.482253
43	1	0	1.196541	-4.805541	-0.913467
44	1	0	1.024205	4.997311	0.444890
45	16	0	2.449647	1.754604	-0.365923
46	16	0	2.501843	-1.745261	0.544917
47	35	0	5.432979	2.683759	-0.605271
48	35	0	5.512847	-2.609448	0.655074

SCF done: -8046.899982 Hartree

No imaginary Frequency.

DFT optimized S0 state geometry of **BDP4**.

Center Number	Atomic Number	Atomic Type	Coordinates (Angstroms)		
			X	Y	Z
1	16	0	-3.762300	4.767457	-0.495901
2	16	0	-3.735034	-4.757095	-0.696106
3	1	0	-4.796843	-1.677786	0.904472
4	1	0	-4.797936	1.615399	0.974745
5	9	0	-3.544965	-0.028079	1.357433
6	9	0	-3.666152	-0.001864	-0.931613
7	7	0	0.178180	-0.004703	0.118151
8	7	0	-1.867694	-1.257936	0.115137
9	7	0	-1.873048	1.240030	0.140516
10	6	0	-5.451487	4.707949	-0.135643
11	1	0	-6.079663	5.560203	-0.354889

12	6	0	-5.813048	3.502506	0.406668
13	1	0	-6.827613	3.264713	0.704652
14	6	0	-3.523916	3.125679	0.101363
15	6	0	-2.189076	2.570684	0.096896
16	6	0	-0.998005	3.330340	0.030153
17	1	0	-0.966242	4.408999	-0.017660
18	6	0	0.090746	2.463385	0.028105
19	6	0	-0.482938	1.141082	0.099719
20	6	0	1.502752	2.822893	-0.021561
21	6	0	1.921765	4.119563	0.337534
22	1	0	1.189494	4.838034	0.693141
23	6	0	3.250067	4.508624	0.279500
24	1	0	3.508076	5.518121	0.574238
25	6	0	4.255126	3.606880	-0.146598
26	6	0	3.837646	2.306382	-0.517379
27	1	0	4.558544	1.581216	-0.874032
28	6	0	2.504830	1.929958	-0.451941
29	1	0	2.225054	0.927041	-0.748753
30	6	0	-5.429069	-4.717439	-0.355604
31	1	0	-6.052399	-5.559802	-0.621833
32	6	0	-5.800655	-3.538802	0.236849
33	1	0	-6.819619	-3.317135	0.532260
34	6	0	-3.509030	-3.145018	-0.020390
35	6	0	-2.176167	-2.587545	0.019044
36	6	0	-0.980612	-3.342247	-0.020780
37	1	0	-0.943048	-4.421716	-0.036074
38	6	0	0.102542	-2.472133	0.067608
39	6	0	-0.478404	-1.153563	0.132802
40	6	0	1.516964	-2.820688	0.087339
41	6	0	2.502307	-1.975929	0.636549
42	1	0	2.206217	-1.021416	1.053662
43	6	0	3.839795	-2.340266	0.668356
44	1	0	4.547845	-1.656887	1.120386
45	6	0	4.277671	-3.579486	0.142992
46	6	0	3.288575	-4.434593	-0.400860
47	1	0	3.563094	-5.396738	-0.814862
48	6	0	1.955606	-4.058022	-0.424278
49	1	0	1.234672	-4.734903	-0.872810
50	5	0	-2.813960	-0.011628	0.153938
51	6	0	-4.715953	-2.644191	0.428505

52	6	0	-4.724331	2.602584	0.542599
53	7	0	5.586652	3.980353	-0.192038
54	7	0	5.613825	-3.938706	0.154277
55	6	0	5.954992	5.368596	0.029413
56	1	0	7.039609	5.465357	-0.031545
57	1	0	5.507973	6.048617	-0.711011
58	1	0	5.648548	5.706551	1.026334
59	6	0	6.569034	3.079067	-0.769356
60	1	0	7.559423	3.528345	-0.686302
61	1	0	6.592603	2.123573	-0.232420
62	1	0	6.377052	2.865197	-1.831536
63	6	0	6.003261	-5.283586	-0.235231
64	1	0	7.088740	-5.372621	-0.178140
65	1	0	5.561439	-6.056531	0.411163
66	1	0	5.707901	-5.498631	-1.268877
67	6	0	6.579349	-3.103834	0.848156
68	1	0	7.576546	-3.526073	0.718077
69	1	0	6.593095	-2.088446	0.435105
70	1	0	6.377198	-3.027082	1.927075

SCF done: -2531.150521 Hartree

No imaginary Frequency.

DFT optimized S0 state geometry of **BDP5**.

Center Number	Atomic Number	Atomic Type	Coordinates (Angstroms)		
			X	Y	Z
1	16	0	-3.219295	4.792746	-0.542111
2	16	0	-3.228412	-4.781234	-0.573950
3	1	0	-4.304563	-1.641121	0.899513
4	1	0	-4.304490	1.634660	0.885750
5	9	0	-3.042647	0.005376	1.339212
6	9	0	-3.148954	-0.006798	-0.951358
7	7	0	0.683446	-0.004046	0.109550
8	7	0	-1.365306	-1.253905	0.127895
9	7	0	-1.363048	1.249913	0.112654

10	6	0	-4.911918	4.738892	-0.211993
11	1	0	-5.530717	5.597182	-0.434664
12	6	0	-5.293222	3.530824	0.314534
13	1	0	-6.314295	3.299873	0.593972
14	6	0	-3.002649	3.142917	0.041643
15	6	0	-1.676237	2.578375	0.050120
16	6	0	-0.473586	3.333412	-0.017757
17	1	0	-0.432154	4.410999	-0.081728
18	6	0	0.601932	2.460511	0.001227
19	6	0	0.025045	1.142632	0.080455
20	6	0	2.023836	2.811899	-0.035296
21	6	0	2.442225	4.074972	0.428729
22	1	0	1.713694	4.758166	0.852370
23	6	0	3.776419	4.452333	0.382556
24	1	0	4.085104	5.425419	0.748844
25	6	0	4.737619	3.566296	-0.133330
26	6	0	4.335606	2.302175	-0.596024
27	1	0	5.076147	1.619803	-0.999294
28	6	0	2.997733	1.932022	-0.547523
29	1	0	2.695223	0.957894	-0.909240
30	6	0	-4.921475	-4.727007	-0.245077
31	1	0	-5.542812	-5.579881	-0.481043
32	6	0	-5.299520	-3.525701	0.299086
33	1	0	-6.320181	-3.295924	0.581010
34	6	0	-3.007586	-3.141926	0.035433
35	6	0	-1.679649	-2.581709	0.055398
36	6	0	-0.477944	-3.339764	0.014441
37	1	0	-0.438117	-4.419320	0.010241
38	6	0	0.598242	-2.468991	0.079593
39	6	0	0.022684	-1.149948	0.135865
40	6	0	2.020026	-2.818329	0.085731
41	6	0	2.987379	-1.990412	0.688891
42	1	0	2.678747	-1.059795	1.147562
43	6	0	4.327039	-2.356817	0.704938
44	1	0	5.062857	-1.715664	1.178363
45	6	0	4.736591	-3.566132	0.118618
46	6	0	3.781654	-4.400268	-0.487880
47	1	0	4.096731	-5.330183	-0.948665
48	6	0	2.445794	-4.026339	-0.501510
49	1	0	1.721241	-4.666280	-0.994062

50	5	0	-2.311701	-0.001348	0.141801
51	6	0	-4.218769	-2.623798	0.459505
52	6	0	-4.215325	2.623059	0.459809
53	6	0	6.116886	3.951132	-0.184644
54	6	0	6.117462	-3.948130	0.137146
55	7	0	7.236209	4.266313	-0.225187
56	7	0	7.238137	-4.260786	0.151124

SCF done: -2447.681046Hartree

No imaginary Frequency.

IV. References

- [1] M. J. Frisch, G. W. Trucks, H. B. Schlegel, G. E. Scuseria, M. A. Robb, J. R. Cheeseman, G. Scalmani, V. Barone, G. A. Petersson, H. Nakatsuji, X. Li, M. Caricato, A. V. Marenich, J. Bloino, B. G. Janesko, R. Gomperts, B. Mennucci, H. P. Hratchian, J. V. Ortiz, A. F. Izmaylov, J. L. Sonnenberg, D. Williams-Young, F. Ding, F. Lipparini, F. Egidi, J. Goings, B. Peng, A. Petrone, T. Henderson, D. Ranasinghe, V. G. Zakrzewski, J. Gao, N. Rega, G. Zheng, W. Liang, M. Hada, M. Ehara, K. Toyota, R. Fukuda, J. Hasegawa, M. Ishida, T. Nakajima, Y. Honda, O. Kitao, H. Nakai, T. Vreven, K. Throssell, J. A. Montgomery Jr., J. E. Peralta, F. Ogliaro, M. J. Bearpark, J. J. Heyd, E. N. Brothers, K. N. Kudin, V. N. Staroverov, T. A. Keith, R. Kobayashi, J. Normand, K. Raghavachari, A. P. Rendell, J. C. Burant, S. S. Iyengar, J. Tomasi, M. Cossi, J. M. Millam, M. Klene, C. Adamo, R. Cammi, J. W. Ochterski, R. L. Martin, K. Morokuma, O. Farkas, J. B. Foresman, D. J. Fox, **2016**.
- [2] P. Jonkheijm, P. van der Schoot, A. P. H. J. Schenning, E. W. Meijer, *Science* **2006**, 313, 80-83.